CLASS VI PERMIT APPLICATION NARRATIVE
40 CFR 146.82(a)

Brown 4 Geologic Sequestration Project

Facility Information

Facility name:	Brown 4 Geologic Sequestration Project Lambda-Brown 4-1 & Lambda-Brown 4-2
Facility contact:	Claimed as PBI [redacted] Claimed as PBI [redacted]
Well location:	Lambda-Brown 4-1: Brown, Manistee County, Michigan 44.3361397, -86.1393888, NAD 27 Lambda-Brown 4-2: Brown, Manistee County, Michigan 44.3418411, -86.1342111, NAD 27

Table of Contents

List of Figures

List of Tables

Project Background and Contact Information

Lambda Energy Resources (Lambda) was formed in 2018 to pursue the acquisition and development of oil and gas resources in the Northern Niagaran Pinnacle Reef Trend (NRT) in Michigan. Lambda owns over 100 individual Niagaran reefs with more than 800 wells and 300,000 net leasehold acres, connected by over 250 miles of Lambda-owned pipeline infrastructure (Figure 1). A comprehensive study conducted by Battelle Memorial Institute estimates that the combined capacity of all individual reefs within the NRT is 230 million metric tonnes of CO_2 sequestration potential, of which Lambda controls the large majority (Kelley et al, 2018).

The reefs within the NRT have proven to be highly effective geologic containers, as evidenced by the multiple reefs utilized for commercial natural gas storage and numerous prior and ongoing Class II CO_2 enhanced oil recovery (EOR) projects.

Lambda plans to adapt existing oil and gas infrastructure to enable the storage of high purity CO_2 captured from multiple carbon-intensive operations, including ethanol plants, cement plants, natural gas processing plants, and future industrial sources with a desire to produce carbon-neutral products. These CO_2 sources will produce low carbon-intensity transportation fuel, cement, natural gas, and products to assist the State of Michigan in achieving its aggressive decarbonization goals.

Within Lambda's extensive portfolio of reefs, the Brown 4 stands out as the optimal first candidate for CO_2 sequestration. The Brown 4 is a depleted gas reef, essentially representing an empty container, ideally suited for permanent CO_2 sequestration (Figure 2). The injection site will consist of two injection wells, Lambda-Brown 4-1 and Lambda-Brown 4-2. In addition to the injection wells, Lambda will convert the two current gas producers in the reef, the Viol 1-4 and the Viol 3-4, to above confining zone monitoring wells prior to injection. These wells will provide continuous measurement of pressure and temperature within the Bass Island Dolomite, the first permeable layer above the A2 Evaporite confining zone. This monitoring will validate the integrity of the primary seal. Additionally, routine collection and analysis of formation samples will be conducted to assess water quality and geochemical properties. This approach enables direct monitoring above the confining layer, facilitating the timely detection of any irregularities.

Lambda will also drill two shallow water wells to monitor and validate the quality of the local drinking water source within the 251-acre Area of Review (AoR). Their primary function will be to verify that CO_2 has not migrated into the USDW due to injection operations.

The Brown 4 Geologic Sequestration Project (GSP) is expected to be ready for service and receiving CO_2 by the 4^{th} quarter 2027. Lambda expects injection operations for this project to last four and half (4.5) years given the expected daily injection volumes, [redacted], and [redacted] of capacity of this reef. Lambda also plans for an additional five years of monitoring and reporting before site closure is completed.

Lambda is not requesting an injection depth waiver or aquifer exemption expansion. There are no federally recognized Native American tribal lands or territories within the proposed AoR.

Figure 1: Distribution of reefs in the NRT.

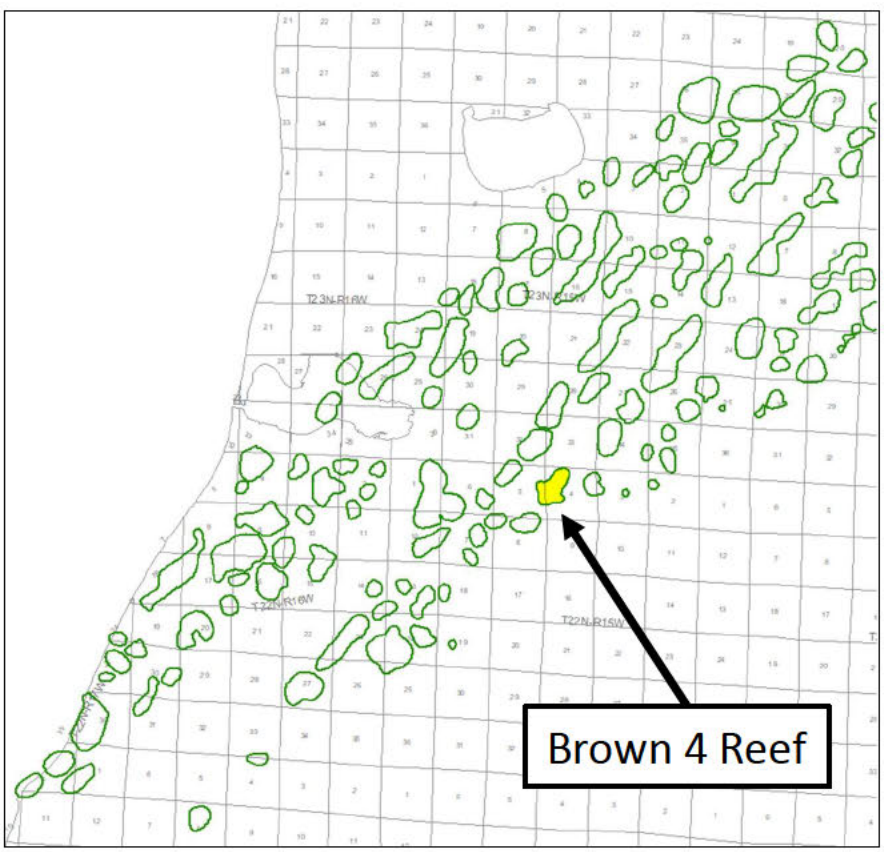

Figure 2: Zoomed in map showing the Brown 4 reef and the surrounding reefs.

Site Characterization

Regional Geology, Hydrogeology, and Local Structural Geology [40 CFR 146.82(a)(3)(vi)]

Niagaran Reef Trend History

The NRT was discovered in 1969, with the majority of development occurring during the 1970 and 1980s, utilizing 2D seismic technology to identify reef locations. The reefs were primarily developed through vertical wells drilled on 80-acre spacing. Lambda acquired its position in the NRT from Merit Energy, which bought the asset from Shell Western E&P Inc, the original developer, in 2001.

Niagaran Reef Trend Geology Overview

The NRT is part of an extensive paleo, shallow shelf carbonate depositional system of hydraulically isolated pinnacle reefs that form a circular belt along the platform margin encircling the Michigan Basin (Figure 3). This system began as a series of coral reefs that formed during the Silurian Period approximately 430 million years ago and is similar to what can now be observed in the Bahamas or Great Barrier Reef along northern Australia (Barnes et al, 2013). Most of the oil and gas producing reefs along the NRT are at depths of approximately 3,500 to 6,500 feet subsea TVD. While individual reef complexes are localized (averaging 50 to 400 acres in area), they may be up to 2,000 acres in areal extent and 150 to 700 feet in vertical relief with the steeply dipping flanks. Reef height, pay thickness, burial depth, and reservoir pressure increase toward the basin center (Gill, 1979). There are approximately 800 reefs in the NRT and approximately 400 in the Southern Niagaran Pinnacle Reef Trend of the Michigan Basin (Barnes et al, 2013). The reef trend was subsequently buried by passive margin deposition of carbonate and evaporite sediments, until the most recent deposition of till sediments during recession of glaciation during the Miocene. Figure 4 shows the stratigraphy above the Niagaran Reef trend.

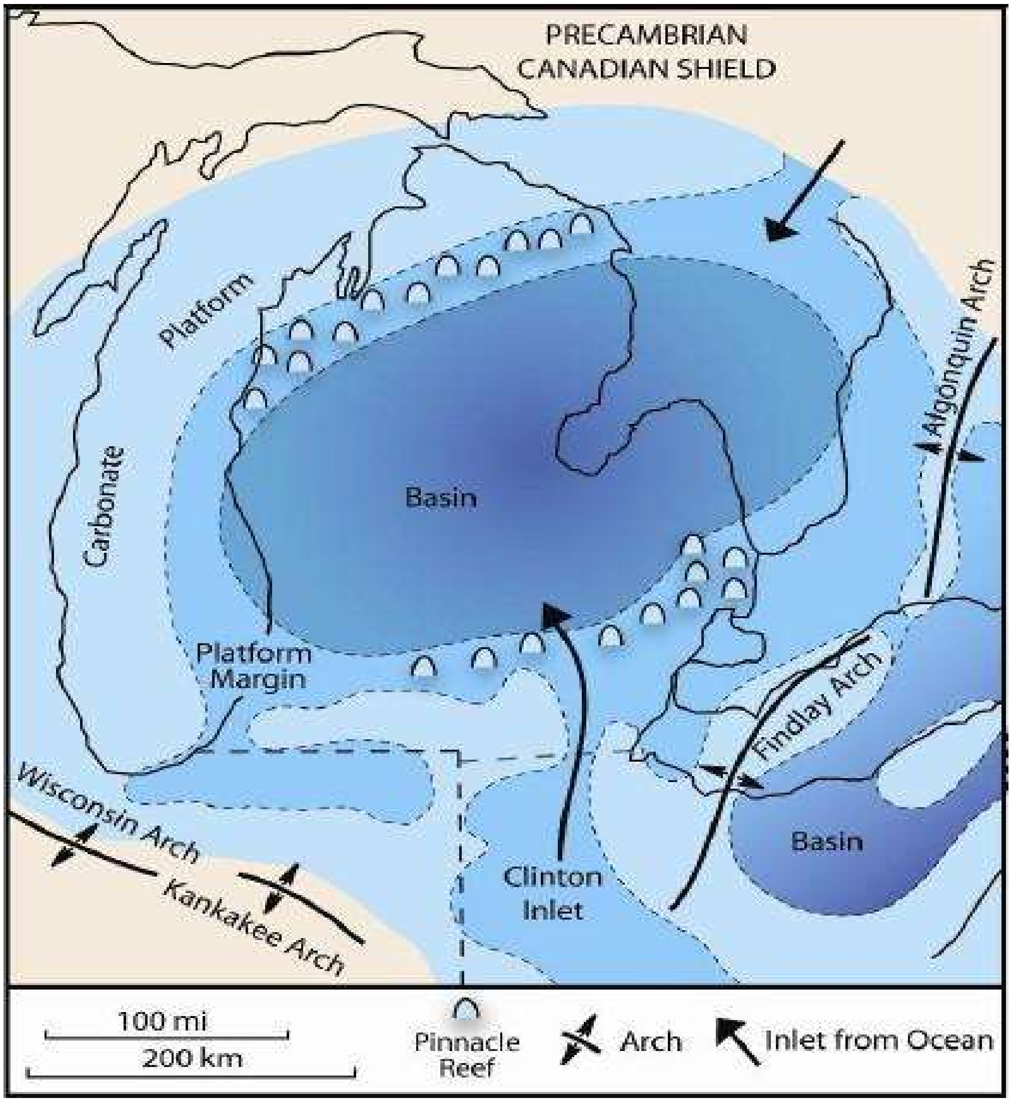

Figure 3: Carbonate platform and basin setting during NRT deposition in Michigan (Briggs and Briggs, 1974)

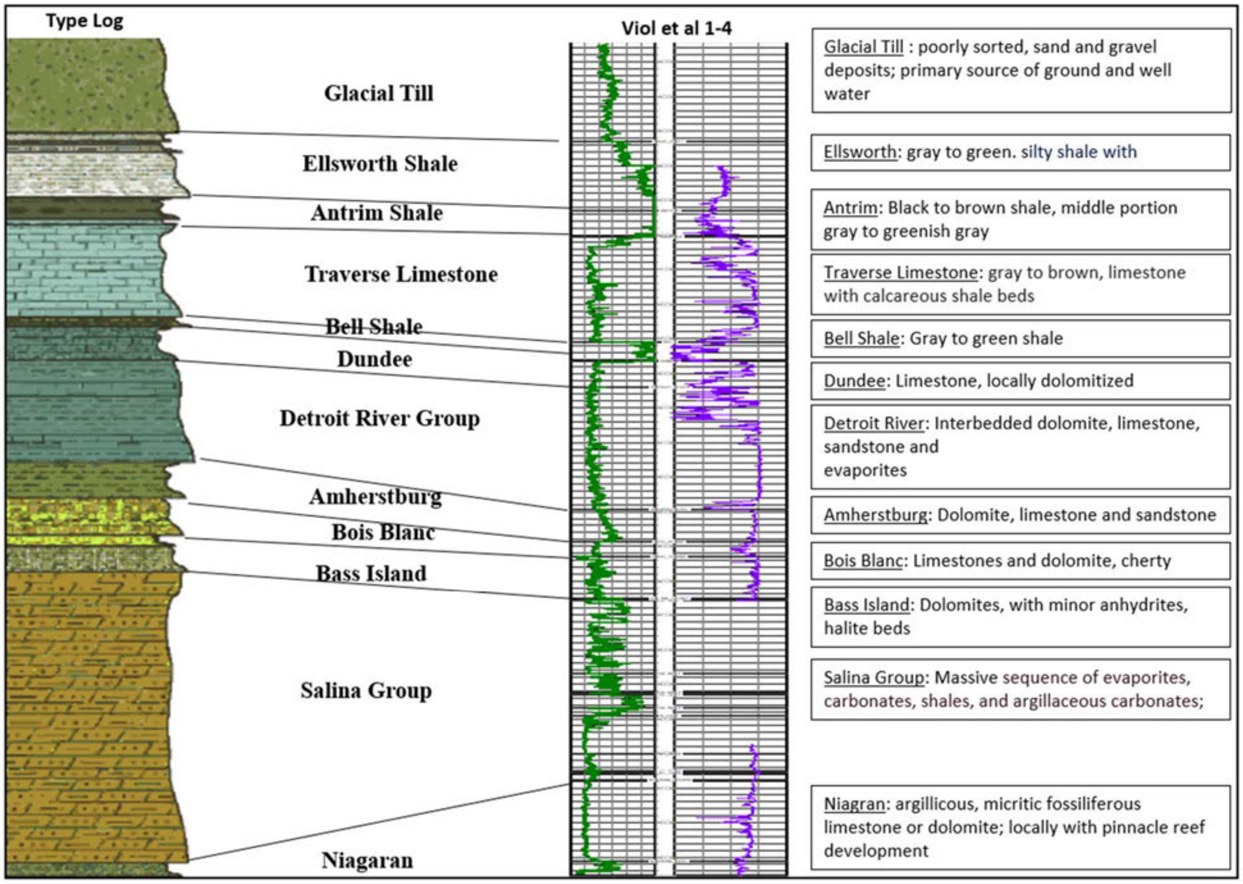

Figure 4: Generalized stratigraphic column above the Niagaran in the NRT.

The reservoir facies primarily consist of porous and permeable dolomite and limestone. Some reefs are completely dolomitized, while others consist predominantly of limestone. Dolomitization of reefs increases as they become shallower, while salt and anhydrite plugging of porosity occurs in the deeper reefs (Gill 1979). Effective porosity intervals for the reservoir range from a few feet to several hundred feet, varying from reef to reef. Porosity values extend to 35 percent, but typically average 3-15 percent. The best porosity and permeability are associated with dolomitized reef core and flank facies. The best reservoir rock is characterized by well-developed inter-crystalline and vuggy porosity, with permeability values of up to several darcies. Secondary porosity can significantly enhance permeability within the reservoir (Core Energy, 2018).

The reef facies developed within the Niagaran Group and includes the Lockport and Guelph lithostratigraphic formations. The Guelph Formation contains the informal units known as the “Gray Niagaran” and the “Brown Niagaran”. The “Brown Niagaran” zone consists of skeletal wackestones, packstones, grainstones, and boundstones/bindstones associated with the carbonate pinnacle reef buildups (Huh 1973). The Guelph Formation comprises the bulk of the reservoir rock associated with the producing reef complex.

The upper seals for the Niagaran reefs are comprised of a sequence of evaporites and/or salt-plugged carbonates which encase the flanks of the reefs and represent the regional seal for the entire reef trend. The A-1 and A-2 Evaporites regionally transition from off-reef salt to anhydrites over the tops of the reef. The A-1 Evaporite (A1E) pinches out on the reef flanks, and the A-2 Evaporite (A2E) forms the primary regional seal for the NRT (Figure 5).

Underlying the A2E is the A1C which belongs to the Ruff Formation. It is a light brown to tan, fine to medium crystalline, laminated, dolomitic mudstone and stromatolitic or microbial laminated boundstones, which may show truncation surfaces and rip-up clasts (Huh 1973; Gill 1973; Ritter 2008). Laminated, dolomitic mudstones occur in inter-reef deposits and on the reef; dolomitic microbial boundstone facies unconformably overlie the Brown Niagaran skeletal deposits (Gill 1973).

The A1C is typically a tight carbonate, however, in some cases, porosity can develop on top of the reef. If reservoir-quality rock is present in the A1C, it is in direct hydraulic communication with the underlying reef and approved by the State of Michigan for comingled production. For this reason, that the A1C is included in the injection interval at the Brown 4 GSP. However, well control from the Brown 4 reef penetrations show that crestal A1C is extremely tight. Figure 6 is a generalized depiction of pinnacle reef reservoir and the overlying carbonates/evaporite seal distribution across the Michigan basin. This a representative example that displays the laterally discontinuous Niagaran Reef reservoir at the reef edge, with limiting features being major evaporite accumulations (>100' thick) and stratigraphic pinchouts (rapid decreases in formation porosity and permeability) that seal the accumulation. Figure 6 shows the relative distribution of reservoir rock and hydrocarbon accumulation seals and their thicknesses in a typical Niagaran Reef. The Bass Island is the first permeable layer above the confining zone.

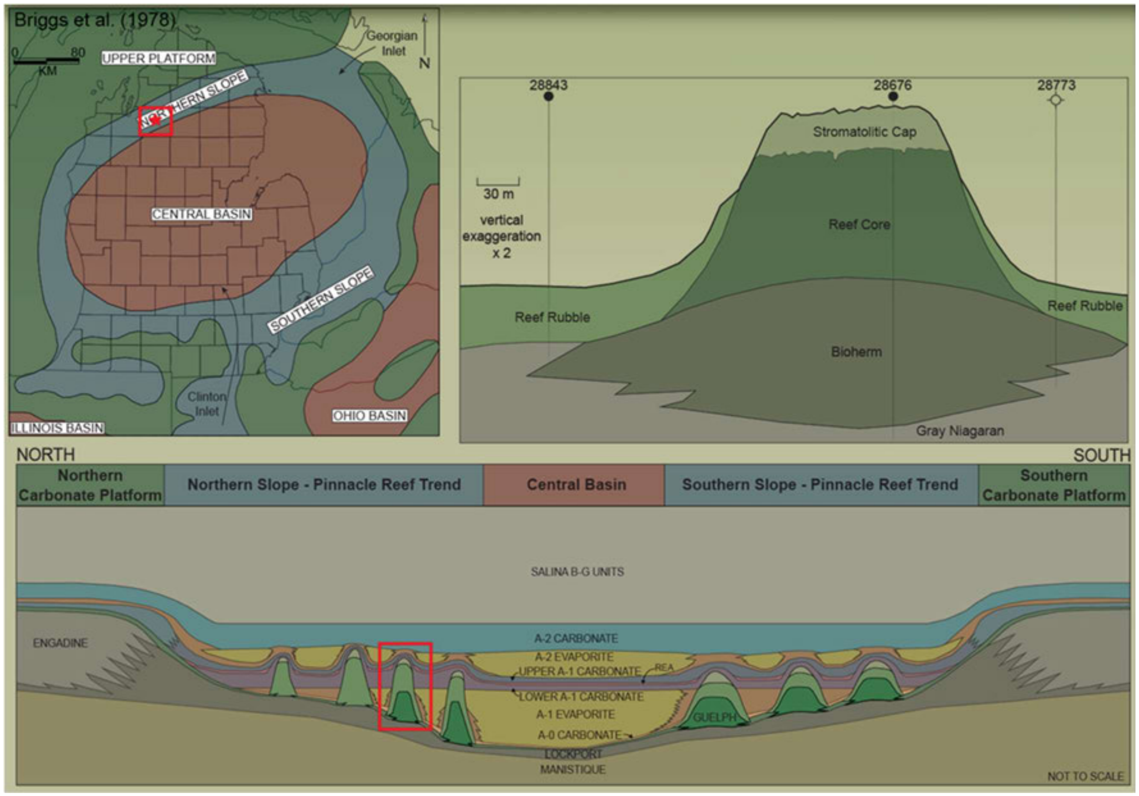

Figure 5: Cartoon relative depiction of pinnacle reef reservoir and overlying carbonates/evaporite seal distribution across Michigan basin (Briggs et al, 1978).

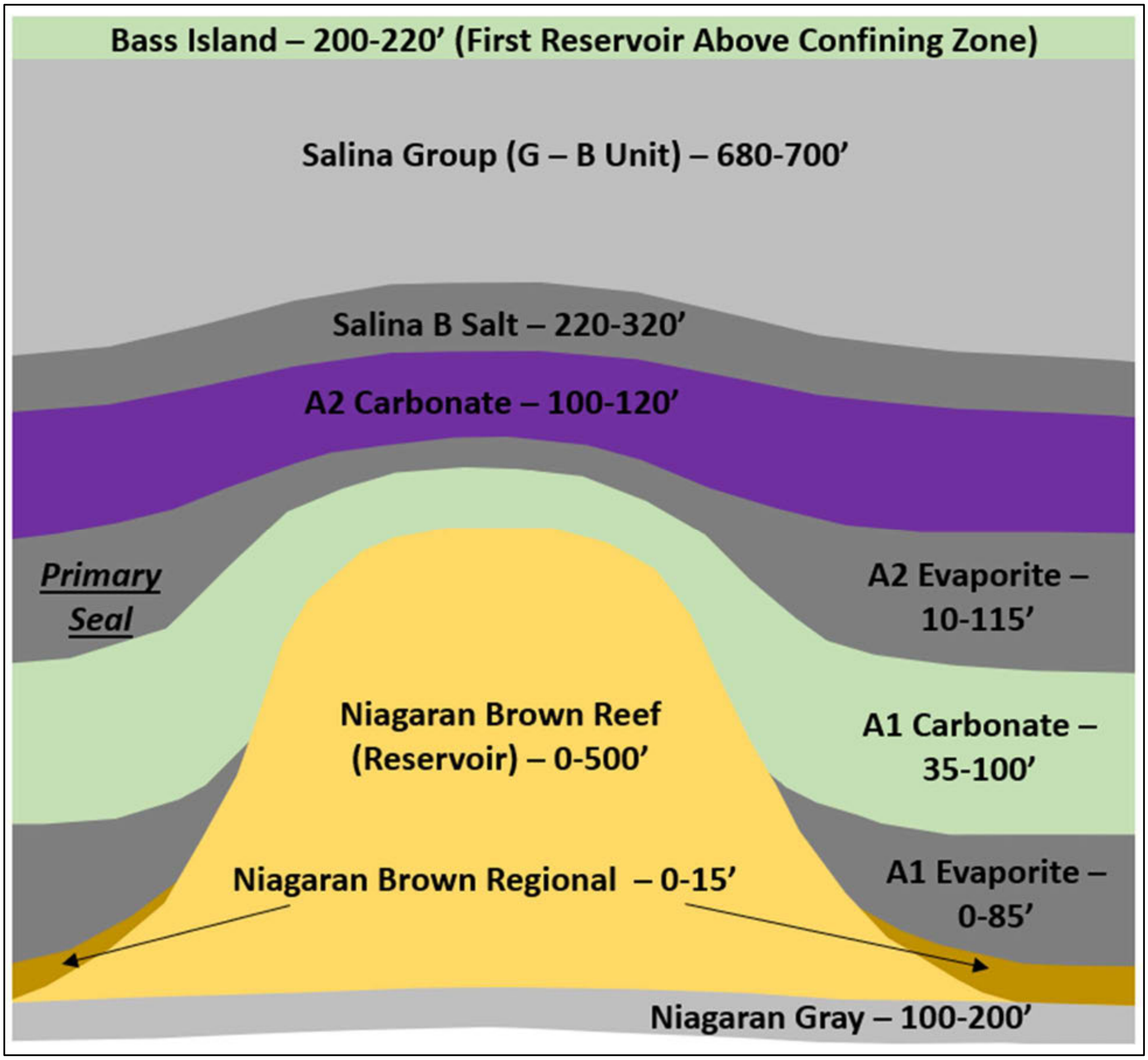

Figure 6: Representative cross section of a reef showing the relative distribution and thickness of formations within the NRT.

NRT Compartmentalization

Each reef within the NRT has been produced for the last 50 years and has been highly depleted from its original reservoir pressure. Within each individual reef, the pressure has declined to its current low pressure, typically less than five percent of the original pressure. This indicates that throughout production history, there has been no outside fluid influx, essentially constituting a long-term negative pressure test.

Multiple reefs are currently utilized for commercial natural gas storage and CO_2 EOR projects. Utilization of the reefs in the NRT for natural gas storage began in 1979, with eight reefs being currently utilized for such purpose.

There are also ten active CO_2 EOR projects in the NRT. Injection and use of CO_2 for EOR projects began in the early 1990's. In 2013 Core Energy LLC, in association with the Midwest Regional Carbon Sequestration Partnership and Battelle Memorial Institute with funding from the US Department of Energy National Energy Technology Laboratory (DOE MRCSP Project #DE-FC26-05NT42589), initiated a project to monitor the injection of approximately 2.8 MMT of CO_2 into multiple reefs. A Monitoring, Reporting, and Verification (MRV) plan (Plan Approval Number 1010117-1) was approved for these projects. As a result, the containment of CO_2 within Niagaran reefs has been proven by independent third parties.

Maps and Cross Sections of the AoR [40 CFR 146.82(a)(2), 146.82(a)(3)(i)]

The Lambda Brown 4 GSP contains one AoR extending over the entire Brown 4 reef outline (Figure 7). The reef outline is well defined by 2D seismic, electric and geophysical logs, and dry hole control. Included in this map are the two proposed injection wells (Lambda-Brown 4-1 and Lambda-Brown 4-2), two confining layer monitor wells (Viol 1-4 and Viol 3-4), and non-reef dry hole plugged wells outside of the AoR. Within the AoR, all pre-existing wells have been identified and a detailed list of these wells has been uploaded to the GSDT tool (Table 1). Lambda utilized Michigan's Oil, Gas, and Minerals Division Data Explorer Dataminer to tabulate all oil and gas wells within the AoR. Figure 8 shows a cross section defining the reef boundary.

Figures 9 through 16 show the locations of all state and federal cleanup sites, surface bodies of water, mines and quarries, water wells, pertinent surface structures, state surface ownership, Tribal surface ownership, roads, and faults, within or nearest to the AoR per § 146.82(a).

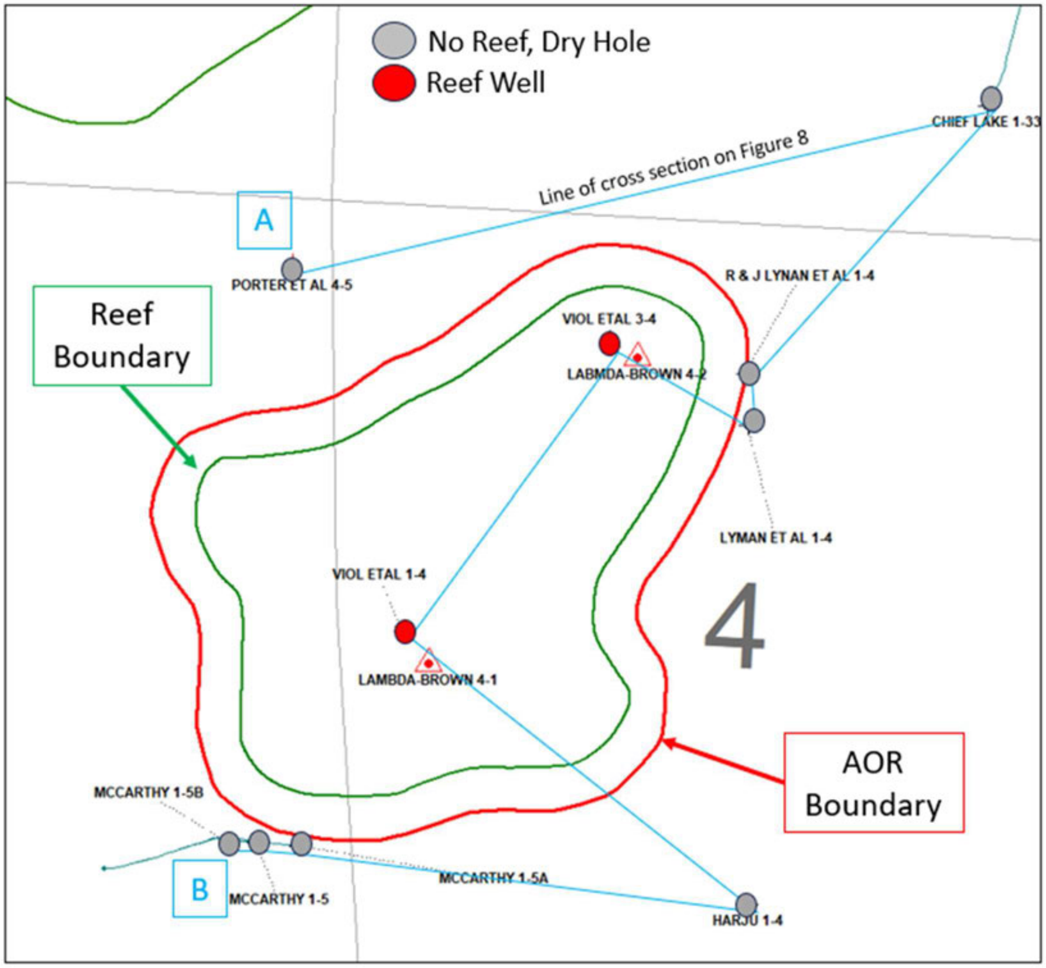

Figure 7: Map showing all wells within AoR boundary and surrounding area that penetrate the confining and sequestration zones.

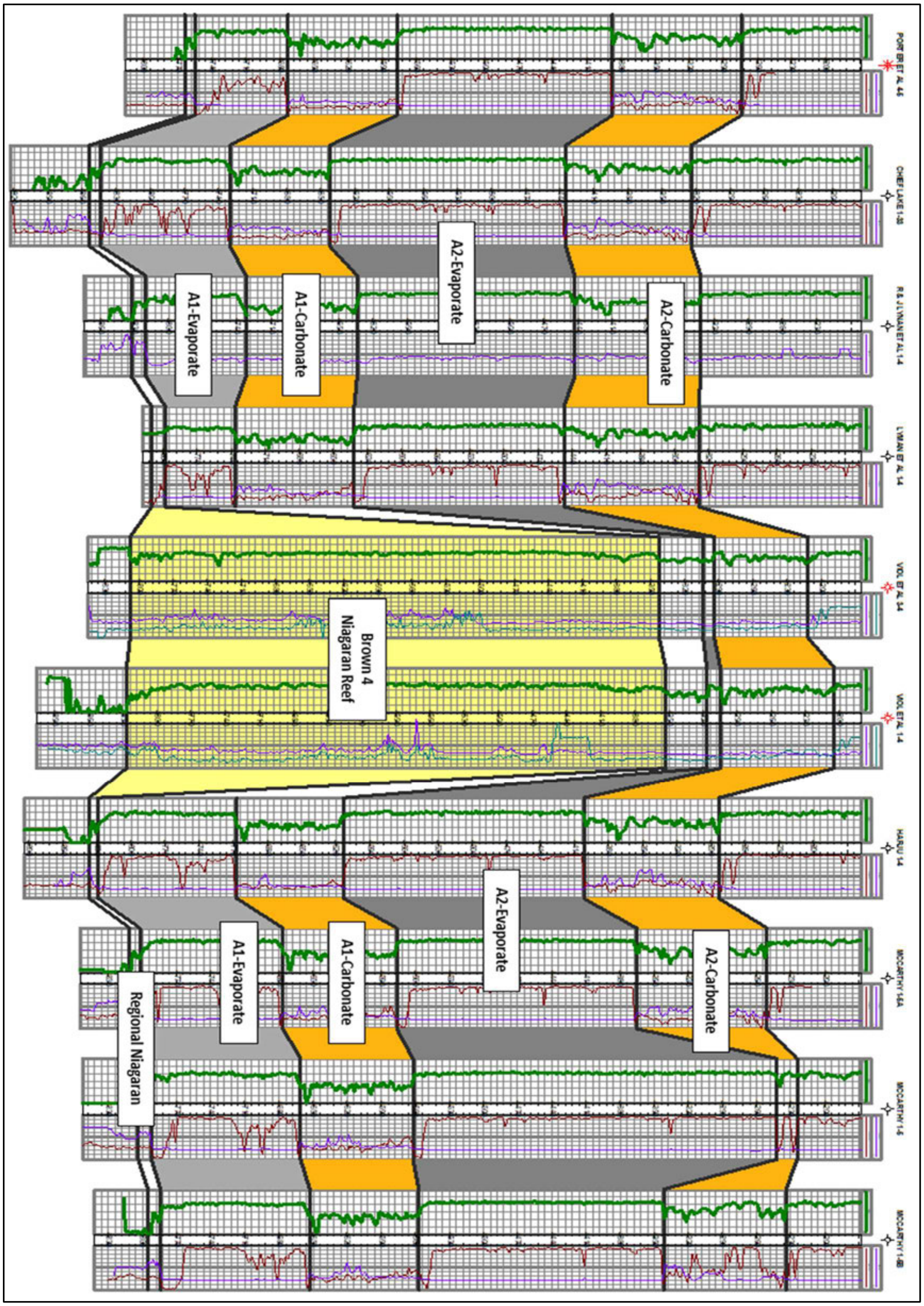

Figure 8: Cross section showing reef and non-reef wells drilled within and adjacent to the Brown 4 GSP.

Table 1: Tabulation of wells within AoR

	Natural Gas Producers	Deep Water Monitor Wells	Injection Wells	USDW Water Wells	USDW Monitor Wells
Current	2	0	0	3	0
Proposed	0	2	2	3	2

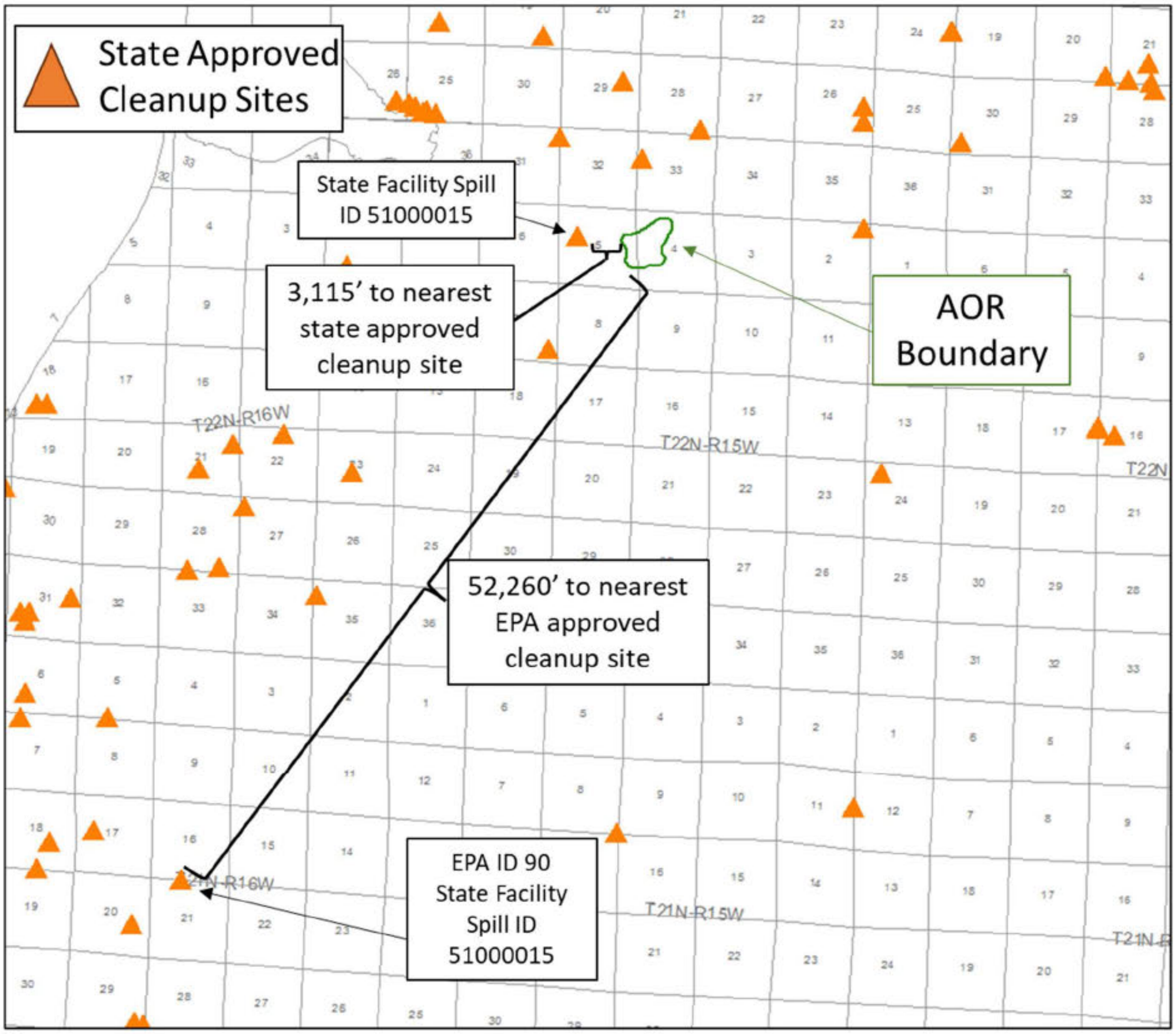

Figure 9: Map of nearest state and federal cleanup sites.

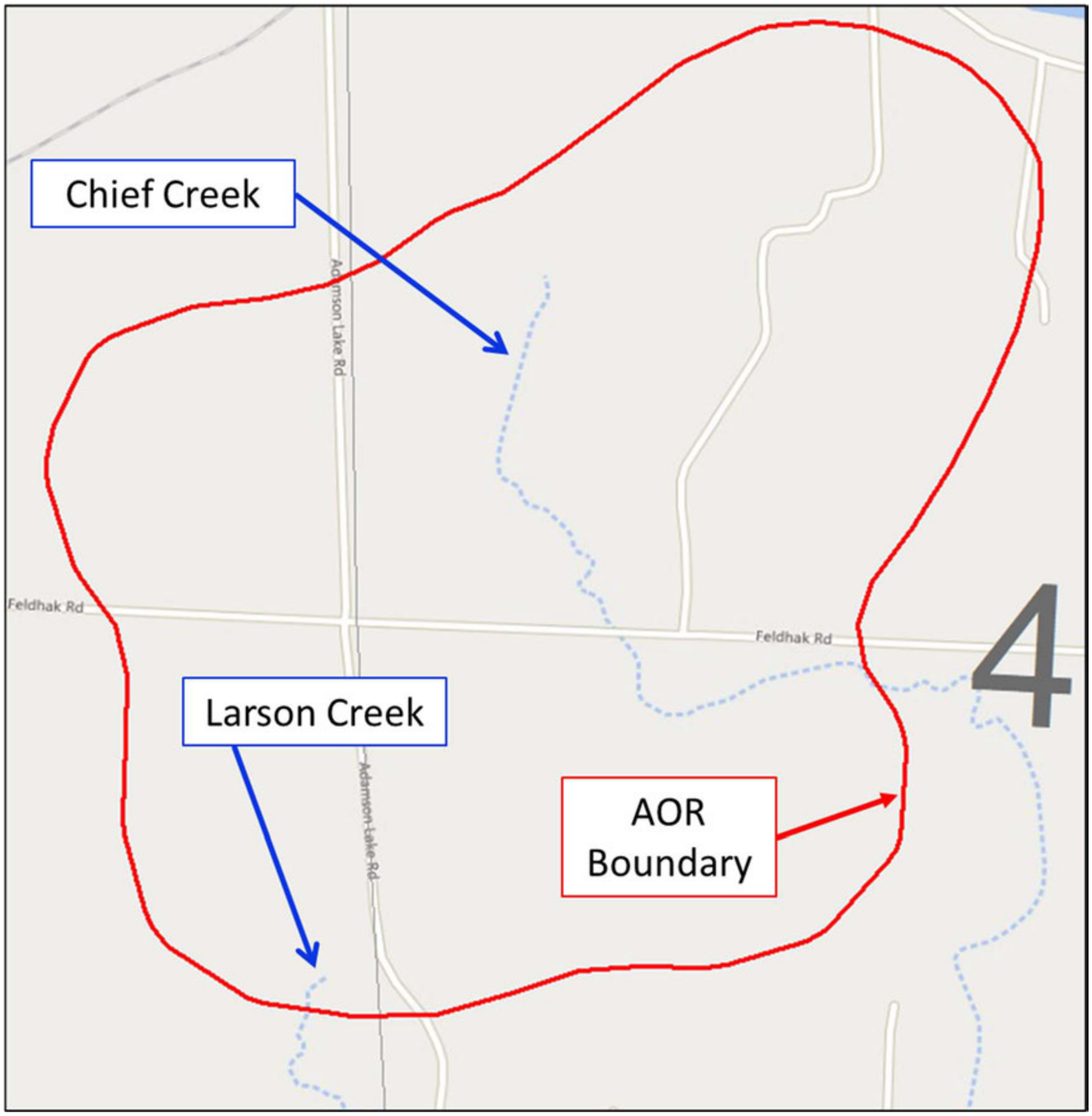

Figure 10: Map of surface bodies of water within AoR.

Figure 11: Map of nearest mines and quarries relative to AoR per Michigan Department of Environment, Great Lakes, and Energy.

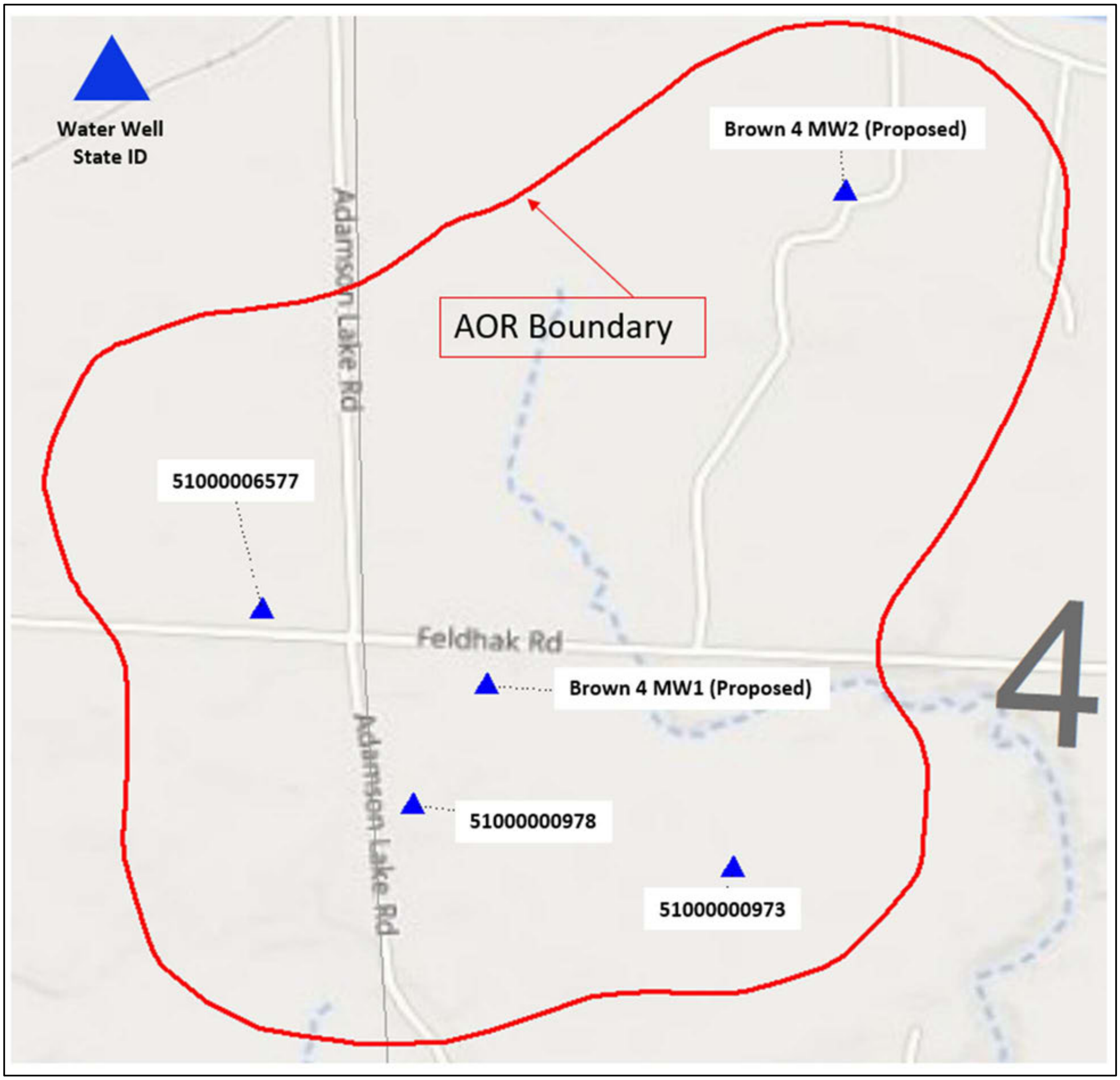

Figure 12: Map of water wells within AoR.

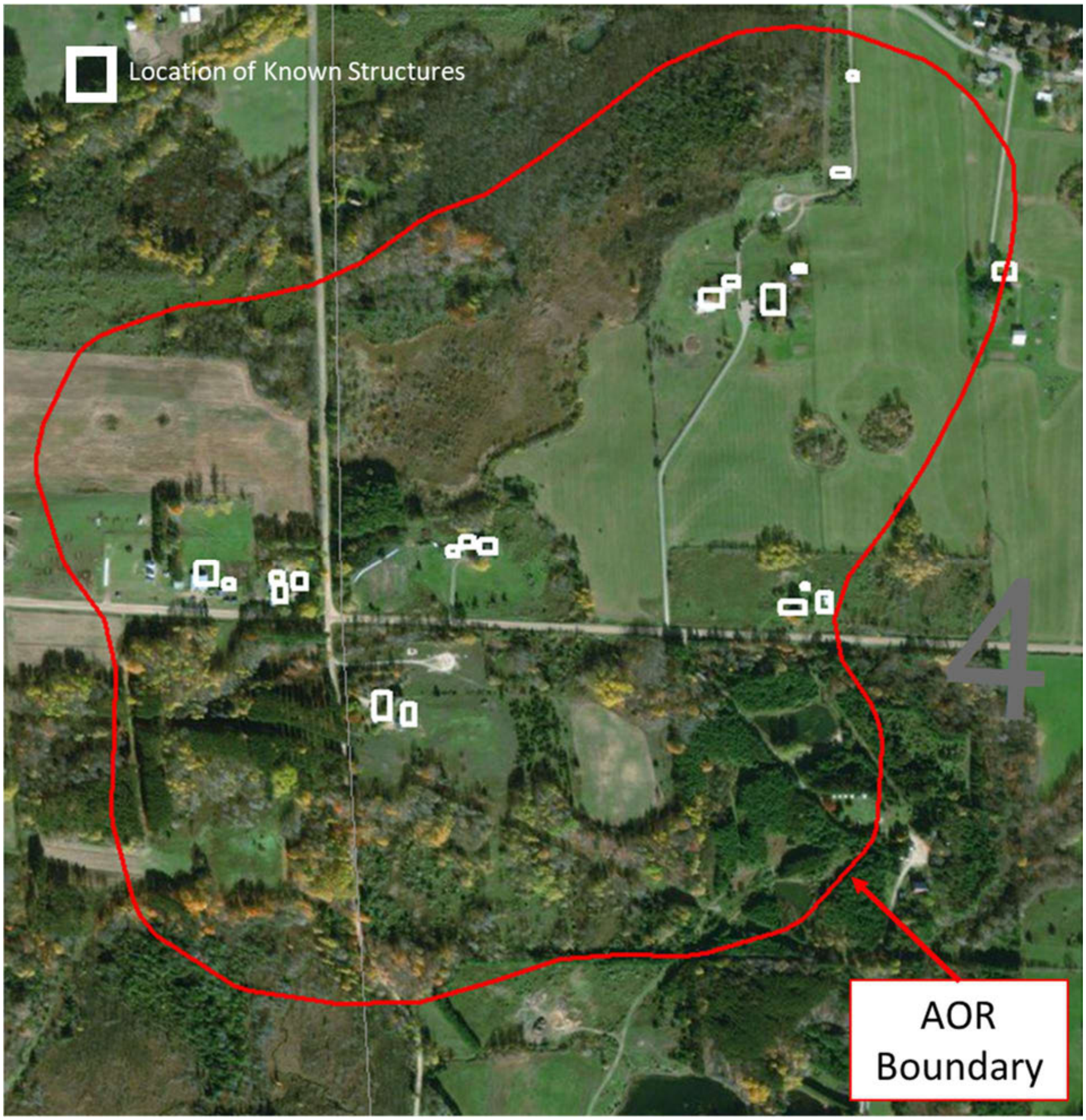

Figure 13: Map of pertinent structures, buildings and homes within AoR.

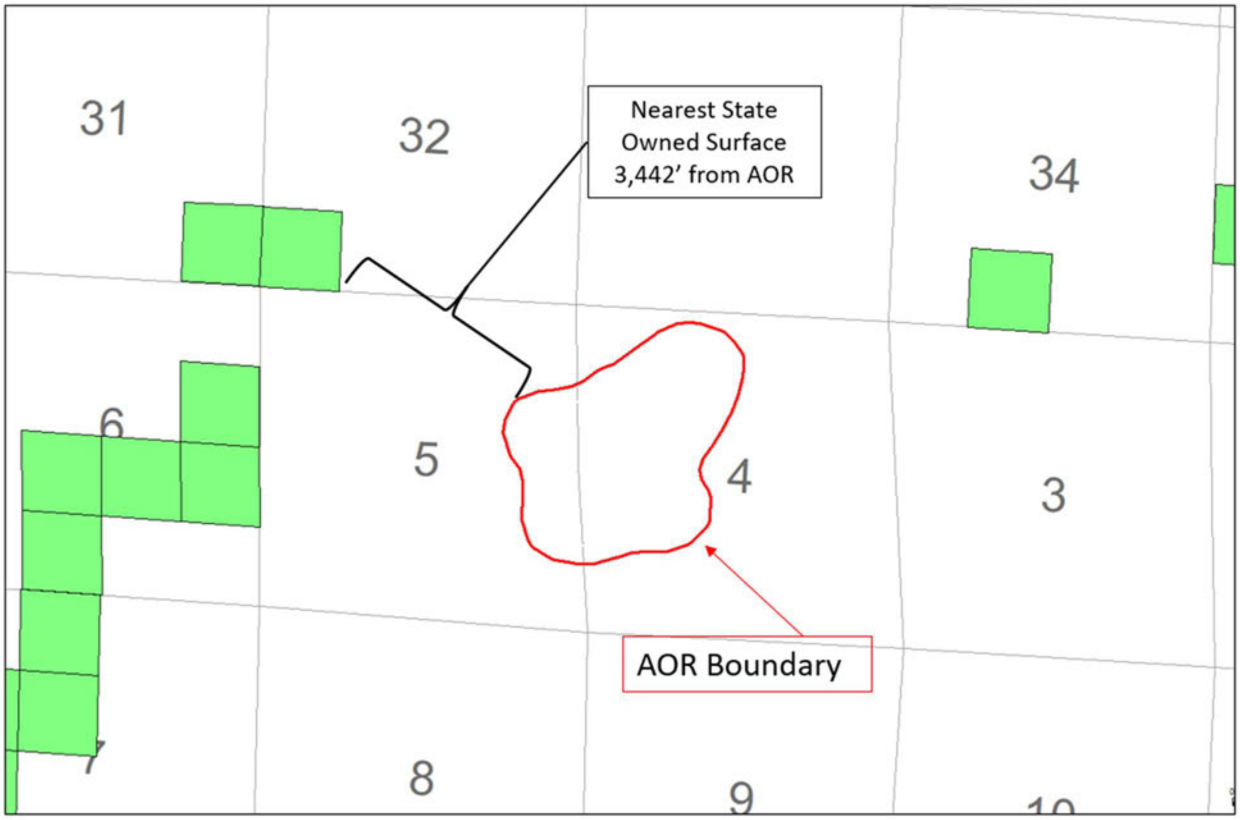

Figure 14: Map of nearest state surface owned land relative to AoR.

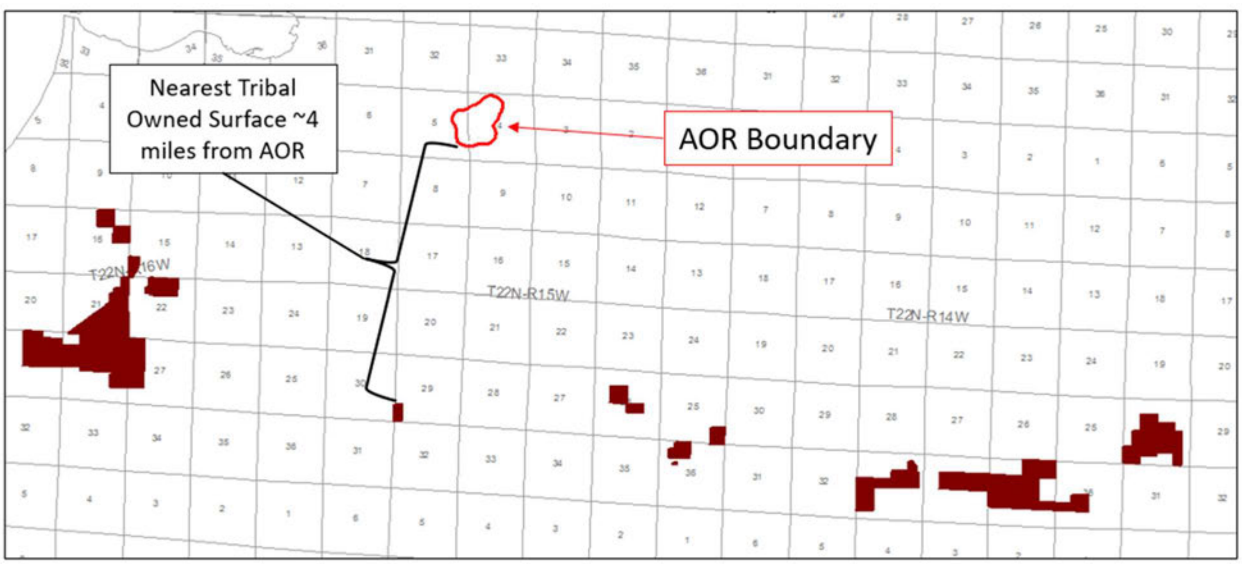

Figure 15: Map of nearest tribal surface owned land relative to AoR.

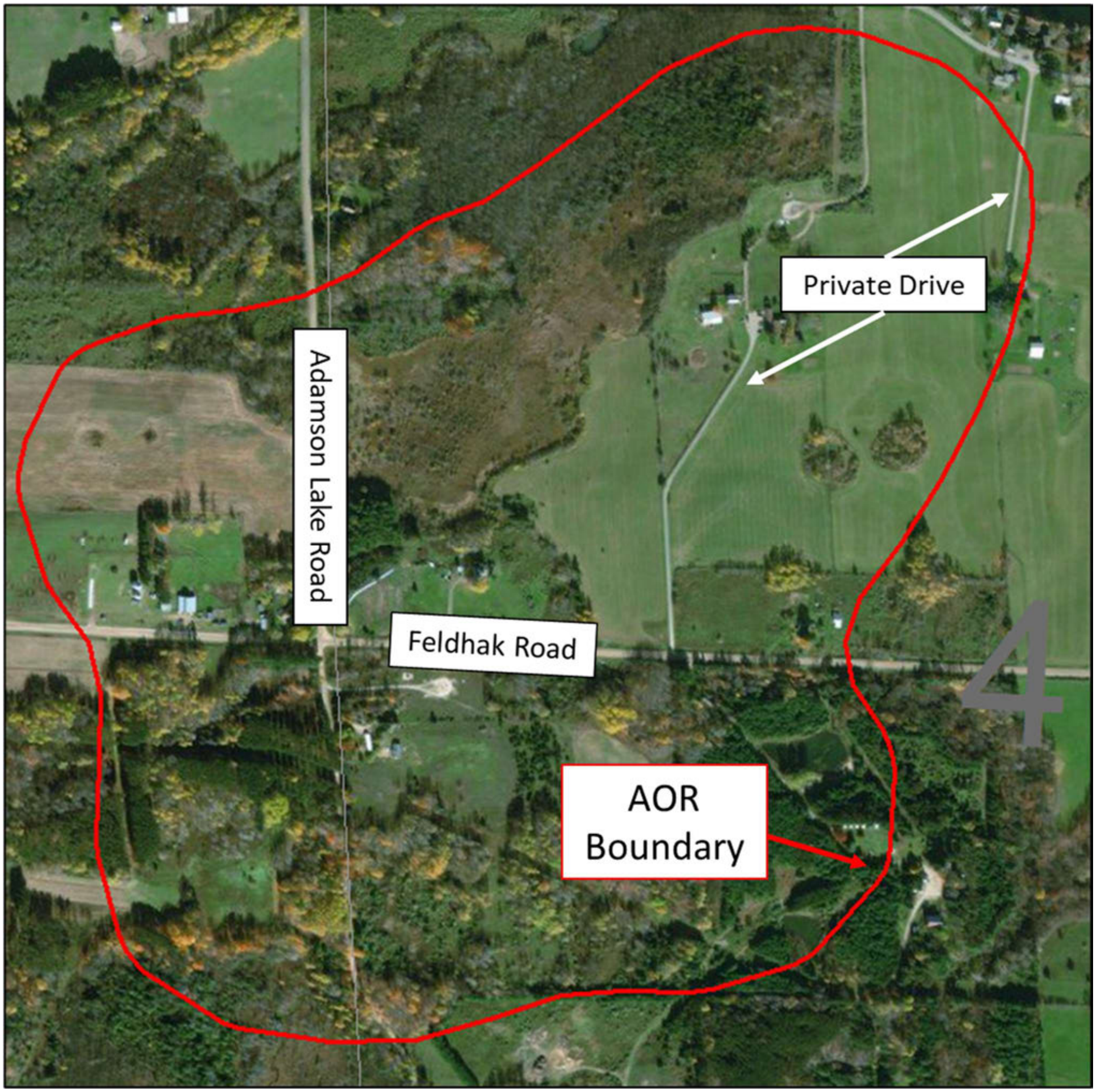

Figure 16: Map of local roads within AoR.

Faults and Fractures [40 CFR 146.82(a)(3)(ii)]

The region exhibits a maximum principal stress plane that trends at a bearing of approximately 30 degrees north of west that results in formation fracturing occurring along this same plane (Gill 1979). Gravity response from aerial gravity surveys confirms this point. Generally, in the NRT, there are very limited instances where faults cut through the reefs. There is no such fault cut instances in the Brown 4 reef, suggesting that faulting and resulting migration are not a risk factor for the GSP (Figure 17).

Claimed as PBI

[redacted]

Figure 17: Gravity survey showing location of faults nearest to the AoR.

Five 2D seismic lines were acquired to evaluate structural features and determine the reef boundary (Figure 18). The comprehensive 2D seismic coverage over the Brown 4 reef also indicates a lack of faulting in the objective formation and adjacent formations. Electric logs from the two penetrations of the objective formation also confirm a lack of faulting. Moreover, it is uncommon for regional pinnacle reefs to have any faulting features due to the nature of their deposition and subsequent lack of tectonic activity.

In instances where the formation is hydraulically fractured, propagation of lateral fractures is expected in the same plane. Lambda does not anticipate induced fracturing or activation of existing faults to occur at the storage complex given the maximum bottomhole injection pressure being limited to initial reservoir pressure of 2,428 psig. The nearest observed fault is approximately eight miles from the Brown 4 AoR. Because of the significant distance between the proposed injection site and the nearest observed fault, the fault does not present a danger to permanent sequestration.

Claimed as PBI

[redacted]

Figure 18: Base map of the Brown 4 reef showing the location of the 2D seismic.

Injection and Confining Zone Details [40 CFR 146.82(a)(3)(iii)]

The Brown 4 reef contained an original accumulation of gas condensate that was the motivation behind its original development. Prior to commercial drilling, which began in January 1974, the reef contained hydrocarbons from a depth of 3,536 feet to 4,046 feet SSTVD with approximately 31 BSCF of original gas in place (OGIP). Brine water populated the remainder of the void pore space at the base of the reef.

In total, the areal extent of the hydrocarbon accumulation in the Brown 4 reef covers 170 surface acres and comprises the geological zone that will sequester CO_2. There are no secondary crude oil or natural gas-bearing objectives above or below the Brown 4 GSP. A cross section for the two wells that penetrate the Brown 4 reef is displayed in Figure 19.

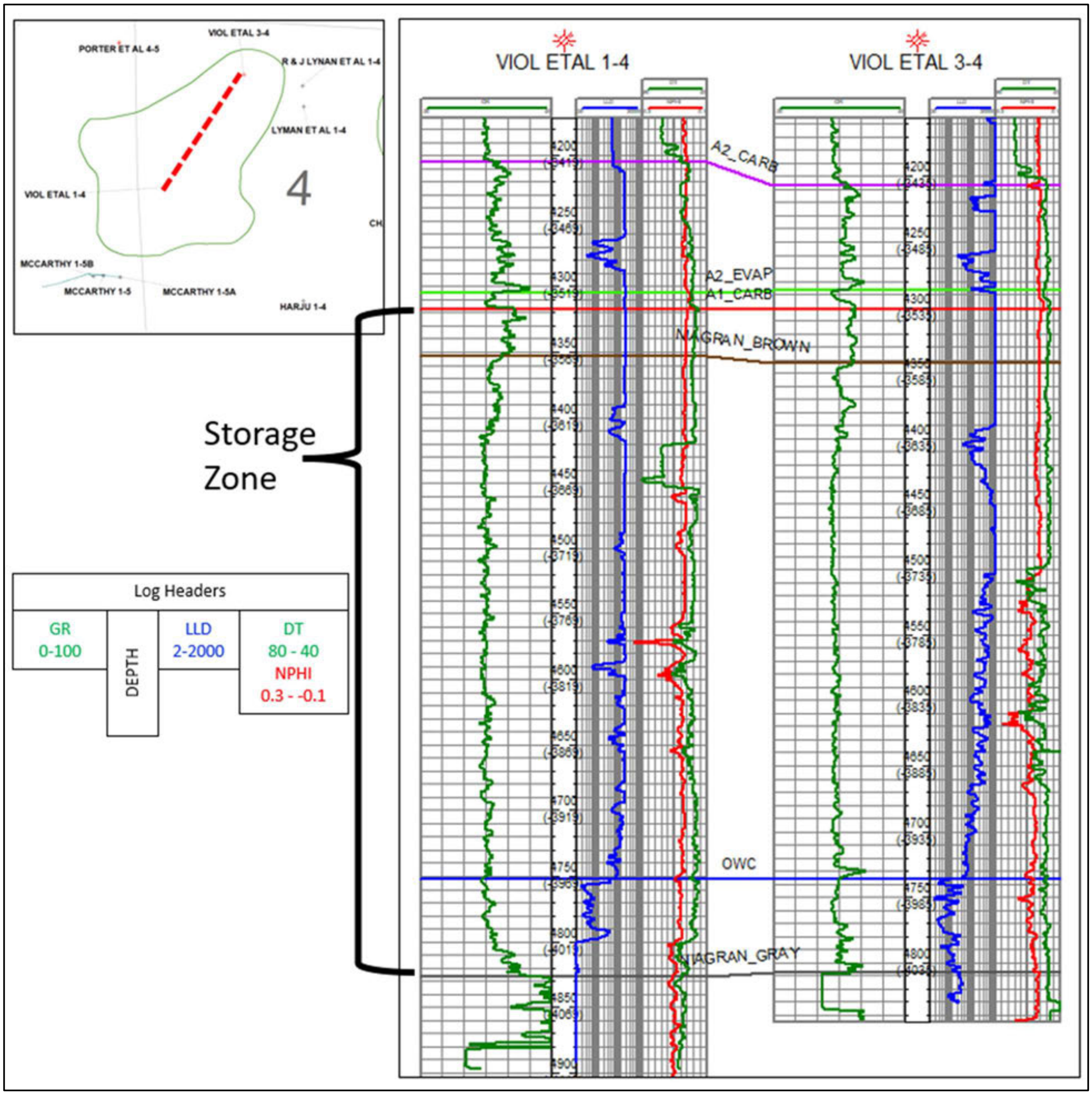

Figure 19: Cross Section of the two wells drilled into the Brown 4 reef, showing the log properties and extent of the storage zone.

Lambda's predecessor, Shell Oil Company, logged the two wells that penetrate the Brown 4 reef. The open-hole log suites acquired after drilling included gamma ray, neutron porosity, sonic porosity, laterolog (resistivity), and micro-laterolog (near-wellbore resistivity / permeability). These logs, combined with regional geologic knowledge, were used to identify and locate the injection and confining zones. Thousands of electric logs and mud logs have been collected in the NRT over the past five decades, providing high confidence in the characterization of both the injection zone and confining zones.

Mineralogy

Based on the petrophysical analysis conducted on the open hole logs in the Viol 1-4 & 3-4 wells, the lithologic descriptions conducted by wellsite geologist during drilling of these wells, and recent X-Ray Diffraction (XRD) analysis, Lambda has high confidence in the lithologic interpretation of the confining and injections zones.

Lambda contracted the Western Michigan University Carbonate Petrology and Characterization Laboratory to conduct an XRD analysis on the cuttings of a nearby well for lithologic characterization of the confining zones. The Gilbert 7-5A XRD analysis was used to confirm the log interpretations of the seal lithology above the sequestration zone. The Gilbert well is located in close proximity to the AoR and has representative log parameters within the seals as those within the AoR. Figure 20 demonstrates that the lithological log interpretations for the B-Salt, A2 Carbonate, and A2 Evaporite (primary confining zone) are consistent with XRD data. The results of the XRD are located in Table 2.

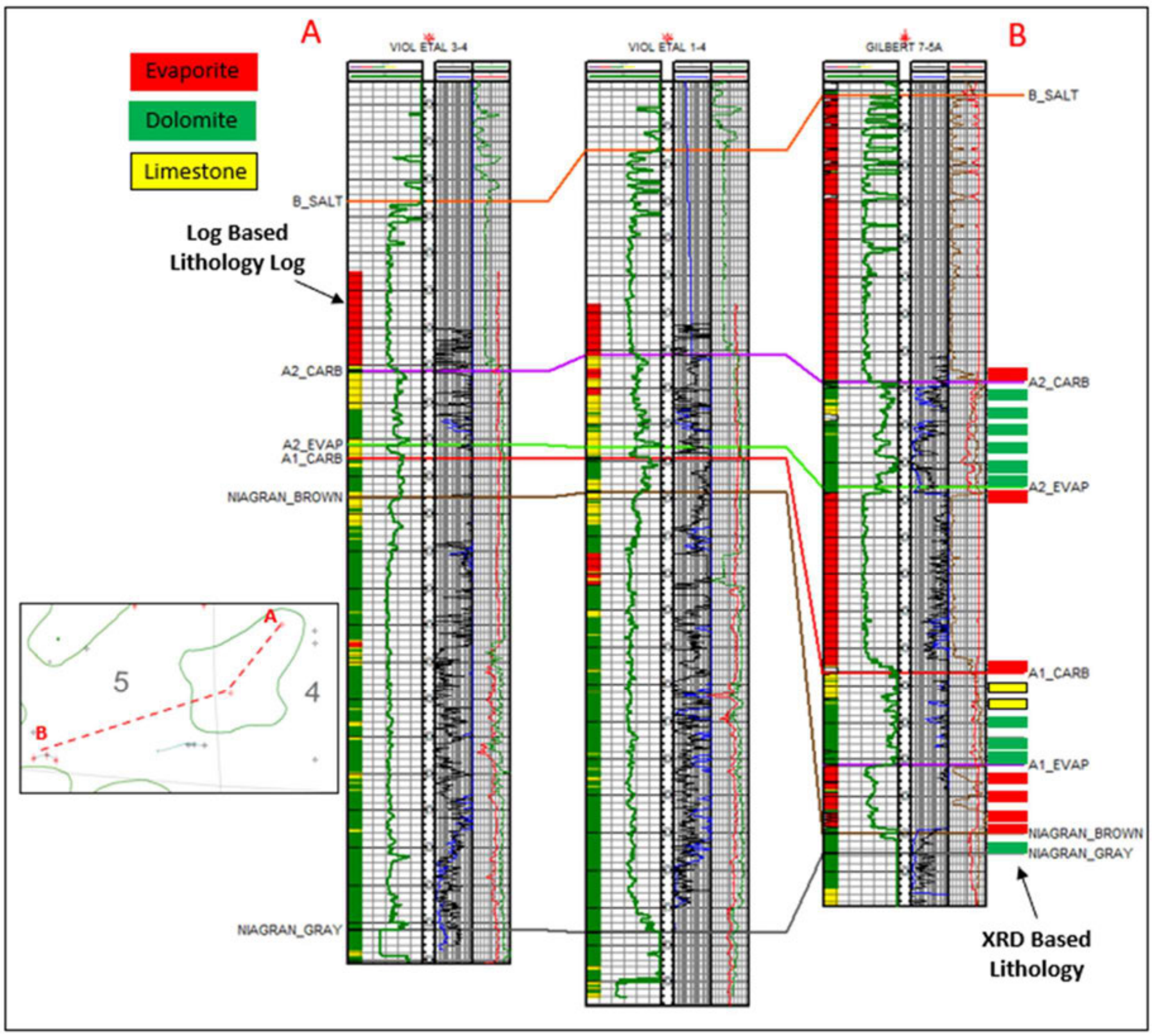

Figure 20: Cross section show the correlation of the Brown 4 reef wells with the Gilbert 7-5A (21101378750100) highlighting the results of the XRD analysis.

Table 2: Laboratory results of x-ray diffraction on well bore cuttings in Gilbert 7-5A well

Claimed as PBI

[redacted]

Porosity and Permeability

After drilling of the Viol 1-4 and Viol 3-4 wells in the Brown 4 reef, wireline log data was acquired with measurements that include but are not limited to gamma ray, borehole caliper, resistivity, micro-lateral, neutron, and sonic logs. A lithology log was created by cross plotting neutron and sonic logs, and was subsequently utilized to generate a lithology corrected formation porosity log. This porosity log was corrected to the core-based porosity by using the transform derived from the Muldavin 2-13 well core analysis. The corrected porosity values were then input into the computational model. The permeability utilized in the computational model was based on the Phi-K transform derived from whole core analysis in the Muldavin 2-13 well.

Claimed as PBI

[redacted]

Figure 21: Cross plot showing the Phi-K Transform calculated from core data from the Muldavin 2-13 well.

Injection Zone: A1-Carbonate/Niagaran Brown

This injection zone has a known reservoir capacity and injectivity as demonstrated by over 40 years of hydrocarbon production history. Injection zone details are noted in Table 3. The well site geologist lithologic descriptions of the injection zone for the Viol 1-4 are shown in Table 4.

Table 3: Injection zone details

Well	Top of Injection Zone TVD (ft)	Base of Injection Zone TVD (ft)	Avg Porosity (%)	Avg Perm (mD)
Viol 1-4	4,316	4,827	6.46	26.3
Viol 3-4	4,300	4,808	6.87	65.6

Table 4: Injection zone well site lithologic description from Viol 1-4 well

Depth	Sample Description
4,316’ – 4,350’	Dolomite; brown, very fine crystalline, trace sucrosic, dense, argillaceous, slightly calcareous
4,350’ – 4,385’	Dolomite; light gray, fine to medium crystalline, fair matrix porosity, abundant oil stain faint cut, some bleeding gas samples
4,385’ – 4,420’	Dolomite; light gray as above, increase in matrix porosity, abundant dead oil stain, samples bleeding gas, as above
4,420’ – 4,444’	Salt filled dolomitic vugs, thin intebeds of dolomite
4,444’ – 4,452’	Salt filled dolomitic vugs, with dolomite as above, thin interbeds
4,452’ – 4,480’	Dolomite; light gray, brown, fine crystalline, no visible porosity, clean
4,480’ – 4,500’	Dolomite; white, medium crystalline sucrosic, rhombic crystals, good matrix and vug porosity, good fluorescence, trace dead oil stain, no cut
4,500’ – 4,545’	Dolomite; gray white, fine crystalline, trace matrix, vug porosity
4,545’ – 4,575’	Dolomite; gray-white, fine to medium crystalline, sucrosic, with rhombic dolomite crystals, trace gilsonite staining – good glow fluorescence
4,575’ – 4,585’	Dolomite; light gray, fine crystalline, decrease in porosity
4,585’ – 4,615’	Dolomite; light gray, medium crystalline, rhombic dolomite crystals, sucrosic, very good matric and vug porosity, abundant dead oil stain, faint to good cut, gilsonite, black bituminous, firm carbonaceous
4,615’ – 4,630’	Dolomite; as above, light gray, some gray dolomite, very fine crystalline, decrease in porosity and fluorescence
4,630’ – 4,670’	Dolomite; light gray-white, fine to medium crystalline sucrosic, with some rhombic dolomite crystal structure, trace dead oil stain, good cut, good fluorescence
4,670’ – 4,685’	Dolomite; predominately white, some light gray, fine to medium crystalline, sucrosic, decrease in porosity and stain and fluorescence
4,685’ – 4,745’	Dolomite; white to gray, very fine crystalline, decreasing porosity, some vug porosity
4,745’ – 4,755’	Dolomite; as above, with some embedded pyrite
4,755’ – 4,800’	Dolomite; light gray, very fine crystalline, hard, dense, clean – trace disseminated pyrite
4,800’ – 4,827’	Dolomite; as above, becoming argillaceous, slightly calcareous

Injectivity

To confirm injectivity of the wells and rock quality of the reef, Lambda utilized Petroleum Experts Prosper software to conduct nodal analysis of each of the Viol wells. Nodal analysis is a production engineering technique that analyzes the performance of a well and determines the rock deliverability (kh). This involves creating a mathematical model of the wells and their associated surface and subsurface components to simulate fluid flow behavior. Lambda integrated bottomhole pressure and flow tests performed at initial production to calibrate the nodal analysis models Inflow Performance Relationship (IPR) curve. The IPR curve represents the relationship between production rate and bottomhole pressure, indicating the wells inflow performance characteristics. After matching the IPR curve, Lambda can accurately model the CO_2 injection rate by calculating the friction down the tubing (VLP curve) for various rates and seeing where the curves cross.

The Lambda-Brown 4-1 Class VI injection well location is adjacent to the Viol 1-4 well and the rock properties of the Lambda-Brown 4-1 are expected to be very similar. The same is true for the Lambda-Brown 4-2 and the Viol 3-4 well. The models were utilized to simulate the behavior of the proposed injectors, running them at various injection and reservoir pressures with all results yielding sufficient injectivity. Figures 22 and 23 below illustrate one case-operating example of the injectors.

Claimed as PBI

[redacted]

Figure 22: Nodal analysis of the Viol 1-4 (i.e. Lambda-Brown 4-1): Claimed PBI [redacted] *reservoir pressure,* Claimed PBI [redacted] *wellhead injection pressure.*

[redacted]

Figure 23: Nodal analysis of the Viol 3-4 (i.e. Lambda-Brown 4-2): [redacted] *reservoir pressure,* [redacted] *wellhead injection pressure*

The point of intersection between the curves delineates the modeled injection capacity. In this case, the Lambda-Brown 4-1 exhibits an injection rate of [redacted], and the Lambda-Brown 4-2 shows a rate of [redacted]. This analysis confirms the high rock quality in this reef and the ability to inject CO_2 at a rate of [redacted].

Primary Confining Zone: A-2 Evaporite

The confining zone above the sequestration formation is comprised of anhydrite, possessing zero porosity and permeability. Subsurface information for the A2E within the AoR is detailed in Table 5. There has been no apparent degradation of the confining zone, ensuring its full ability to seal any vertical fluid movement. The lithologic description of the confining zone from the Viol 1-4 well, provided by the well site geologist, is shown in Table 6. The A2E is widely acknowledged as the primary confining zone for all reefs within the NRT, exhibiting lateral continuity across the area, as depicted in Figure 24.

Table 5: A2 Evaporite subsurface data

Well	Top of Confining Zone TVD (ft)	Base of Confining Zone TVD (ft))	Avg Porosity (%)	Avg Perm (mD)
Viol 1-4	4,303	4,316	0%	0
Viol 3-4	4,286	4,300	0%	0

Table 6: A2 Evaporite well site lithologic description from Viol 1-4 well

Depth	Sample Description
4,303' – 4,316'	**A2 Evaporite:** Anhydrite with dolomite, gray-brown, very fine crystalline, hard, dense, argillaceous, anhydritic

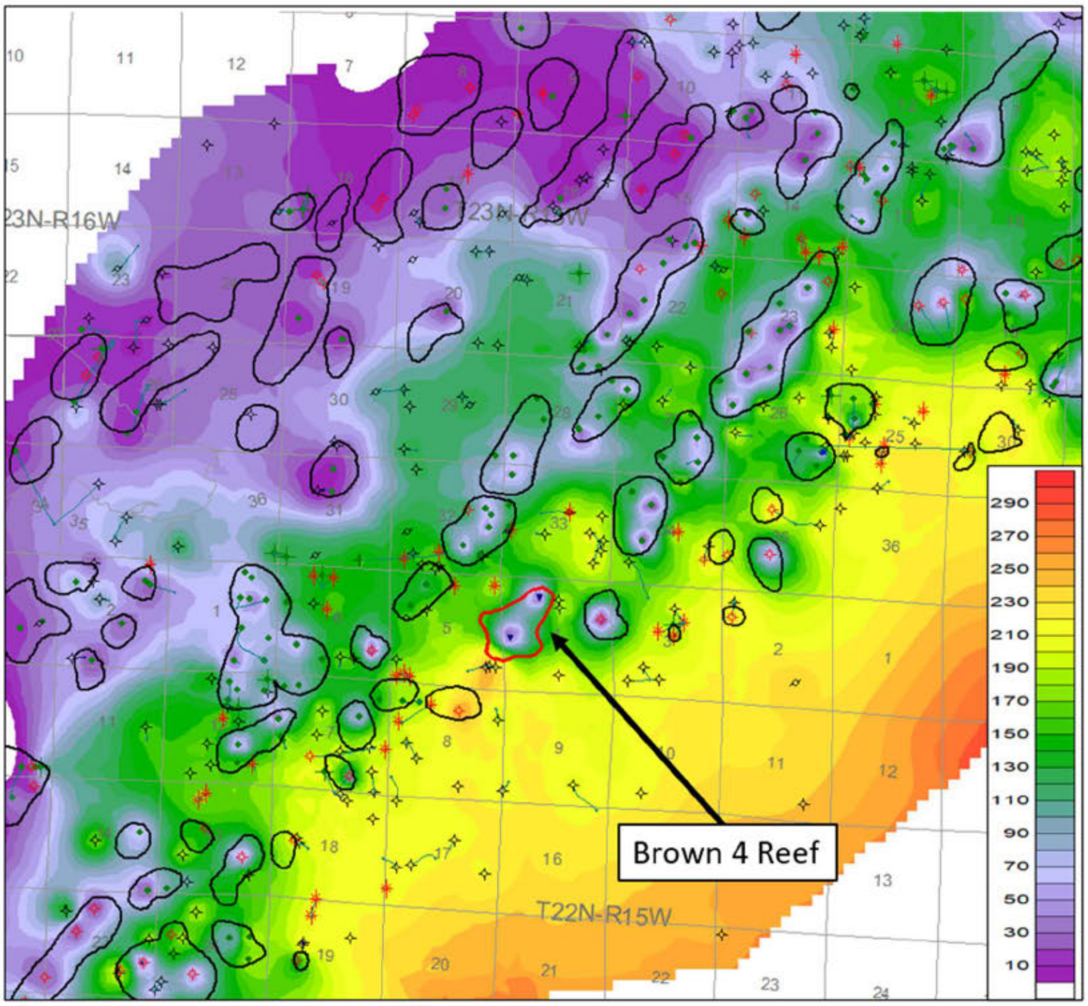

Figure 24: Isopach map of the A2 Evaporite showing consistent deposition across the region.

Secondary Confining Zone: B-Salt

The B-salt represents a secondary confining zone above the sequestration formation. This formation is a massive depositional salt with zero porosity and permeability. There are approximately 200 feet of B-salt above that act as an additional trapping mechanism for the storage complex. The base of the B-salt lies approximately 100 feet above the top of the primary confining zone, the A2E. The subsurface data of this formation are shown in Table 7. There has been no apparent degradation of the confining zone, and it has full ability to seal any vertical fluid movement. The well site geologist lithologic description from the Viol 1-4 well of the confining zone is shown in Table 8.

Table 7: B-Salt subsurface data

Well	Top of Confining Zone TVD (ft)	Base of Confining Zone TVD (ft)	Avg. Porosity (%)	Avg Perm (mD)
Viol 1-4	3,986	4,205	0%	0
Viol 3-4	4,033	4,210	0%	0

Table 8: B-Salt well site lithologic description from Viol 1-4 well

Depth	Sample Description
3,986' – 4,190'	**B-Salt:** Salt, with occasional stringer of shale, gray-green and red and dolomite, very fine crystalline, gray, tan and brown
4,190' – 4,205'	**B-Salt**: Dolomite, gray brown, very fine crystalline, hard dense argillaceous, with trace shale gray silty

Geomechanical and Petrophysical Information [40 CFR 146.82(a)(3)(iv)]

Lithological properties were determined using standard geophysical log analysis techniques from the Viol 1-4 and Viol 3-4 wells. Electric and mud log analyses have been performed in the NRT throughout the past five decades, providing high confidence in the characterization of both the injection and confining zones.

Testing has also been conducted within the NRT to determine stress and fracture characteristics of different reefs as part of integrated CO_2 sequestration efforts from other operators. The testing was done for the primary purpose of ensuring conformance with guidelines established under the Underground Injection Control (UIC) program, which limits the operating conditions under which CO_2 may be injected to take place below the apparent fracture pressure.

One specific study was performed by a consortium led by Battelle Memorial Institute, with Baker Hughes as the wellsite service provider, and Core Energy, LLC as the operator. A 2019 publication in the American Rock Mechanics Association (ARMA) publication from Raziperchikolaee et al (2019) describes the wholly similar geologic setting in Otsego County, Michigan, including a single depleted pinnacle reef as the objective storage target, and completed testing to ultimately determine the orientation and magnitude of minimum horizontal stress. The study describes how minimum horizontal stress changes with CO_2 injection due to the 'poroelastic' effect of injection. The final resulting fracture gradient of the Niagaran Brown formation in the aforementioned study was found utilizing three separate methods:

1) Pressure decline analysis using the isolated interval pressure vs. square root of shut-in time (De Bree and Walters, 1989);

2) Log-Log pressure decline analysis using the pressure derivative of the delta pressure and delta time in log-log plot (Jones and Sargeant, 1993);

3) G-function analysis by plotting the isolated interval pressure vs G-time plot (Castillo, 1987; Barree et al, 2007).

The following information was drawn from a third-party report by Frac Diagnostics, LLC, commissioned by Lambda for the purposes of determining fracture initiation pressure in the injection and confining zones of the Brown 4 GSP.

Frac Diagnostic's approach to determine the fracture initiation pressure for the Brown 4 reef first utilizes the rock properties and tectonic stress elements found in the ARMA report to calibrate the model. Next, an industry-leading commercial fracture simulation software, FRACPRO, was used to 'history match' the fracture characteristics of the subject zones from the well in the referenced paper. The Viol 1-4 and Viol 3-4 e-line logs were used to construct the mechanical earth model in terms of depth correlation to the CO_2 storage zone. The findings in Lambda's geomechanical study allow it to estimate the potential for fracturing out of the injection zone into the bounding layers during CO_2 injection with a high degree of confidence.

Lambda rock analysis study evaluated fracture pressures at the original Brown 4 reef reservoir pressure of 2,428 psig, which will be the maximum bottomhole injection pressure. The third-party study from Frac Diagnostics is summarized in the section below.

Fracture Potential of Target Zones

The process of delineating the pressures required to initiate a fracture within the Brown 4 sequestration zone is addressed below. In this study, a conservative approach has been taken and is based on stress estimates calculated using the equation below.

$$\boxed{\sigma_{H,min} = \frac{\nu}{1-\nu}\left(\sigma_V - \alpha P_p\right) + \alpha P_p + \sigma_{ext}}$$

Equation 1: Minimum horizontal stress relationship

In the relationship above, ν is the Poisson's Ratio, σ_v is the overburden stress, α is the Biot's constant, P_p is the reservoir pressure, (ranged from 10 to 2,428 psig), and σ_{ext} is the Tectonic stress influence (Raziperchikolaee et al, 2019). A "layman's view" of this relationship is that a fracture can be created when the applied pressure overcomes combined effect of rock properties, the reservoir pressure, the load from the overburden, and regional tectonics. The minimum horizontal stress is the closure stress of the formation. After calculating the closure stress, the breakdown pressure (or "fracture initiation pressure") in each interval was estimated using Equation 2, which is the lower-limit estimate for breakdown pressure in a vertical wellbore.

$$P_{BD} = \frac{3\sigma_{H,min} - \sigma_{H,max} + T - \alpha\left(\frac{1-2\nu}{1-\nu}\right)P_p}{2(1-\nu)}$$

Equation 2: Pressure breakdown relationship

In this second relationship, several variables ($\sigma_{H,min}$, ν, α, and P_p) have been defined previously. In Equation 2, $\sigma_{H,max}$ represents maximum horizontal stress, and T represents the rock tensile strength. The maximum horizontal stress was estimated by adding tectonic stress (a product of the Young's modulus multiplied by tectonic strain). Values for tensile strength and tectonic strain were assumed following an iterative analysis which calibrated the breakdown gradients in the Niagaran Brown interval to data presented in Raziperchikolaee et al (2019). The final calculations used a value of [redacted] for tensile strength and applied a tectonic strain of [redacted]. It is important to note here, that both the breakdown pressures and the minimum closure pressures were calibrated to the well in the ARMA paper.

Mechanical Earth Model

To estimate the pressures required to create a fracture, it is important to build a Mechanical Earth Model. Plainly stated, this is a numerical representation of the rock layers in terms of their mechanical properties, their porosity, and other aspects as they affect the fracture initiation pressures. Table 9 summarizes the Mechanical Earth Model (MEM) for the Viol 1-4. This table is input into FRACPRO.

Table 9: MEM for the Viol 1-4 at a 2,428 psig reservoir pressure in the relevant zones

True Vertical Depth (ft)	Layer Thickness (ft)	Lithology Layer	Young's Modulus (MMpsi)	Poisson's Ratio	Breakdown (Fracture) Pressure (psi)	Breakdown (Fracture) Gradient (psi/ft)
[redacted]	[redacted]	[redacted]	[redacted]	[redacted]	[redacted]	[redacted]
[redacted]	[redacted]	[redacted]	[redacted]	[redacted]	[redacted]	[redacted]
[redacted]	[redacted]	[redacted]	[redacted]	[redacted]	[redacted]	[redacted]
[redacted]	[redacted]	[redacted]	[redacted]	[redacted]	[redacted]	[redacted]
[redacted]	[redacted]	[redacted]	[redacted]	[redacted]	[redacted]	[redacted]

This table shows the pressures required to initiate a fracture in each layer. If the injection pressure is less than these estimated pressures, a fracture will not be initiated. The bottomhole injection pressure would need to be greater than [redacted] to initiate a fracture within the storage reservoir. The bottomhole injection pressure would need to be greater than [redacted] to breach containment of the A2 Evaporite. The same workflow is applied to the sequestration and confining layers of the Viol 3-4, and the results are shown in Table 10.

Table 10: MEM for the Viol 3-4 at a 2,428 psig reservoir pressure in the relevant zones

True Vertical Depth (ft)	Layer Thickness (ft)	Lithology Layer	Young's Modulus (MMpsi)	Poisson's Ratio	Breakdown (Fracture) Pressure (psi)	Breakdown (Fracture) Gradient (psi/ft)
[redacted]	[redacted]	[redacted]	[redacted]	[redacted]	[redacted]	[redacted]
[redacted]	[redacted]	[redacted]	[redacted]	[redacted]	[redacted]	[redacted]
[redacted]	[redacted]	[redacted]	[redacted]	[redacted]	[redacted]	[redacted]
[redacted]	[redacted]	[redacted]	[redacted]	[redacted]	[redacted]	[redacted]
[redacted]	[redacted]	[redacted]	[redacted]	[redacted]	[redacted]	[redacted]

Management of injection pressure based on guidelines set forth by Lambda and noted in Testing and Monitoring section will prevent initiation of a fracture within the injection zones. Lambda utilized the fracture initiation calculations from this geomechanical report as a constraint in the reservoir simulation model to ensure target injection rates can be achieved without approaching fracture initiation pressure. Note that the maximum bottomhole injection pressure is 2,428 psig, which is approximately [redacted] below the injection zone fracture initiation pressure.

Seismic History [40 CFR 146.82(a)(3)(v)]

There has not been a meaningful naturally caused seismic event in the NRT over the last 140 years of recorded history, with the two recorded events being derived from mining activities. A map of seismicity in Michigan reveals no major earthquakes proximal to the Brown 4 AoR storage complex, with the nearest seismic activity near Dewitt, MI on September 9, 1994 (Figure 25). The full list of seismic activity in Michigan per the United States Geologic Survey is listed in Table 11. The AoR (and entire NRT) is also located in the zone designated as the "lowest" risk by the USGS in their long-term model with a seismicity that would not cause a catastrophic loss of containment (Figure 26). In addition to the information presented above showing no historical seismic activity in the region, no faulting is observed on the 2D seismic data.

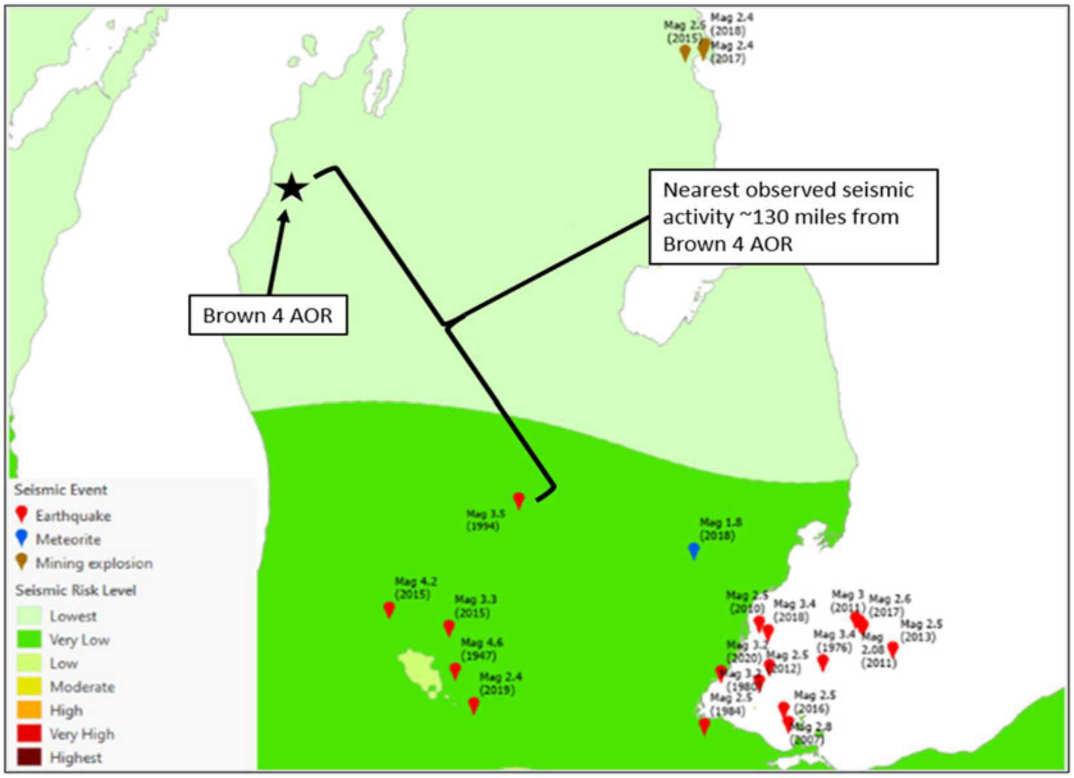

Figure 25: Map of Seismic Activity in Michigan (USGS).

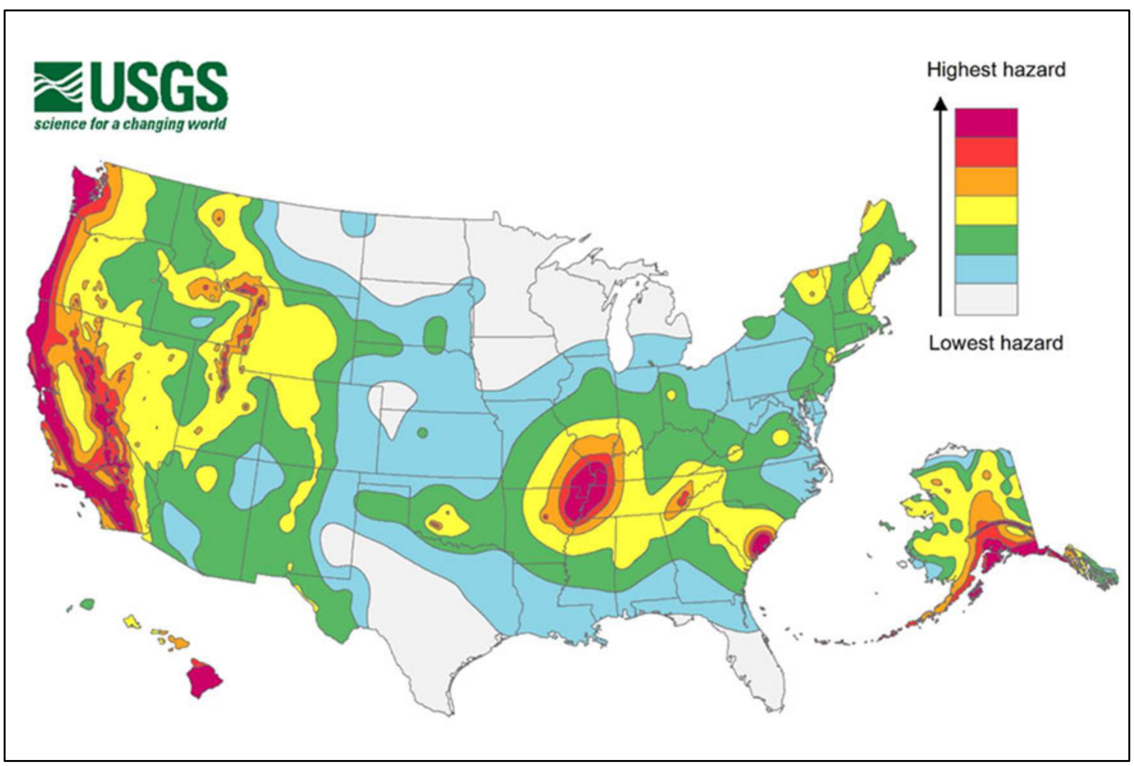

Figure 26: 2018 Long-term National Seismic Hazard Map (USGS).

Table 11: Seismic activity in Michigan

Date	Latitude	Longitude	Magnitude	Mag Type	Place	Type
2022-07-11	41.8158	-83.5123	2.4	ml	5 km W of Luna Pier, Michigan	Earthquake
2022-05-23	42.8995	-82.4453	2.5	ml	2 km NNW of Corunna, Canada	Earthquake
2020-08-21	41.9125	-83.3179	3.2	mwr	2 km SSE of Detroit Beach, Michigan	Earthquake
2019-04-03	41.7532	-84.8845	2.4	ml	4 km WNW of Clear Lake, Indiana	Earthquake
2018-05-07	45.1078	-83.3691	2.4	mb_lg	7 km NE of Alpena, Michigan	Mining Explosion
2018-04-20	42.1181	-83.015	3.4	mwr	Michigan	Earthquake
2018-01-17	42.538	-83.481	1.8	ml	0 km N of Walled Lake, Michigan	Meteorite
2017-12-18	45.0828	-83.3808	2.4	ml	4 km ENE of Alpena, Michigan	Mining Explosion
2017-05-14	42.136	-82.41	2.6	mb_lg	18 km ENE of Leamington, Canada	Earthquake
2016-02-07	41.6503	-82.8969	2.5	ml	6 km W of Put-in-Bay, Ohio	Earthquake
2015-06-30	42.1464	-85.0459	3.3	mb_lg	5 km NNE of Burlington, Michigan	Earthquake
2015-05-02	42.2357	-85.4285	4.2	mwr	5 km S of Galesburg, Michigan	Earthquake
2015-02-16	45.0744	-83.502	2.5	mb_lg	5 km WNW of Alpena, Michigan	Mining Explosion
2013-02-17	42.018	-82.224	2.5	mblg	31 km E of Leamington, Canada	Earthquake
2012-09-07	41.864	-83.076	2.5	mblg	17 km ESE of Stony Point, Michigan	Earthquake
2011-02-24	42.1745	-82.4553	2.08	ml	18 km NE of Leamington, Canada	Earthquake
2011-02-23	42.157	-82.43	3	mblg	18 km NE of Leamington, Canada	Earthquake
2010-03-08	42.163	-83.07	2.5	mblg	7 km ENE of Grosse Ile, Michigan	Earthquake
2007-04-12	41.722	-82.924	2.8	mblg	11 km NW of Put-in-Bay, Ohio	Earthquake
1994-09-02	42.798	-84.604	3.5	mblg	5 km SSW of DeWitt, Michigan	Earthquake
1984-01-14	41.645	-83.427	2.5	md	4 km E of Oregon, Ohio	Earthquake
1976-02-02	41.96	-82.67	3.4	lg	11 km SSW of Leamington, Canada	Earthquake

Hydrologic and Hydrogeologic Information [40 CFR 146.82(a)(3)(vi), 146.82(a)(5)]

The primary freshwater aquifers in this region are located within the group of formations known as the 'Glacial Drift'. The stratigraphic cross section shown in Figure 27 shows the relative depth of the USDW to Brown 4 reef. The map in Figure 28 shows the maximum depth of the base of Glacial Drift is approximately 800 feet, while the top of the Brown 4 Reef is approximately 4,300 feet, allowing approximately 3,500 ft of vertical separation between the deepest USDW zone and the injection zone (Table 12). Most drinking water wells in the area typically range in depth from 50 – 250 feet and drinking water wells within the AoR range from 80-120 feet deep. Figure 29 is a cross section depicting the drinking water wells and injection zone within the AoR. The measurements of groundwater depths from surrounding drinking water wells were used to determine that groundwater flow in the AoR was to the south-southwest (Figure 30). Lambda plans to drill two shallow groundwater monitoring wells to monitor geochemical changes in the USDW. The proposed locations will be immediately adjacent to the Class VI injection wells.

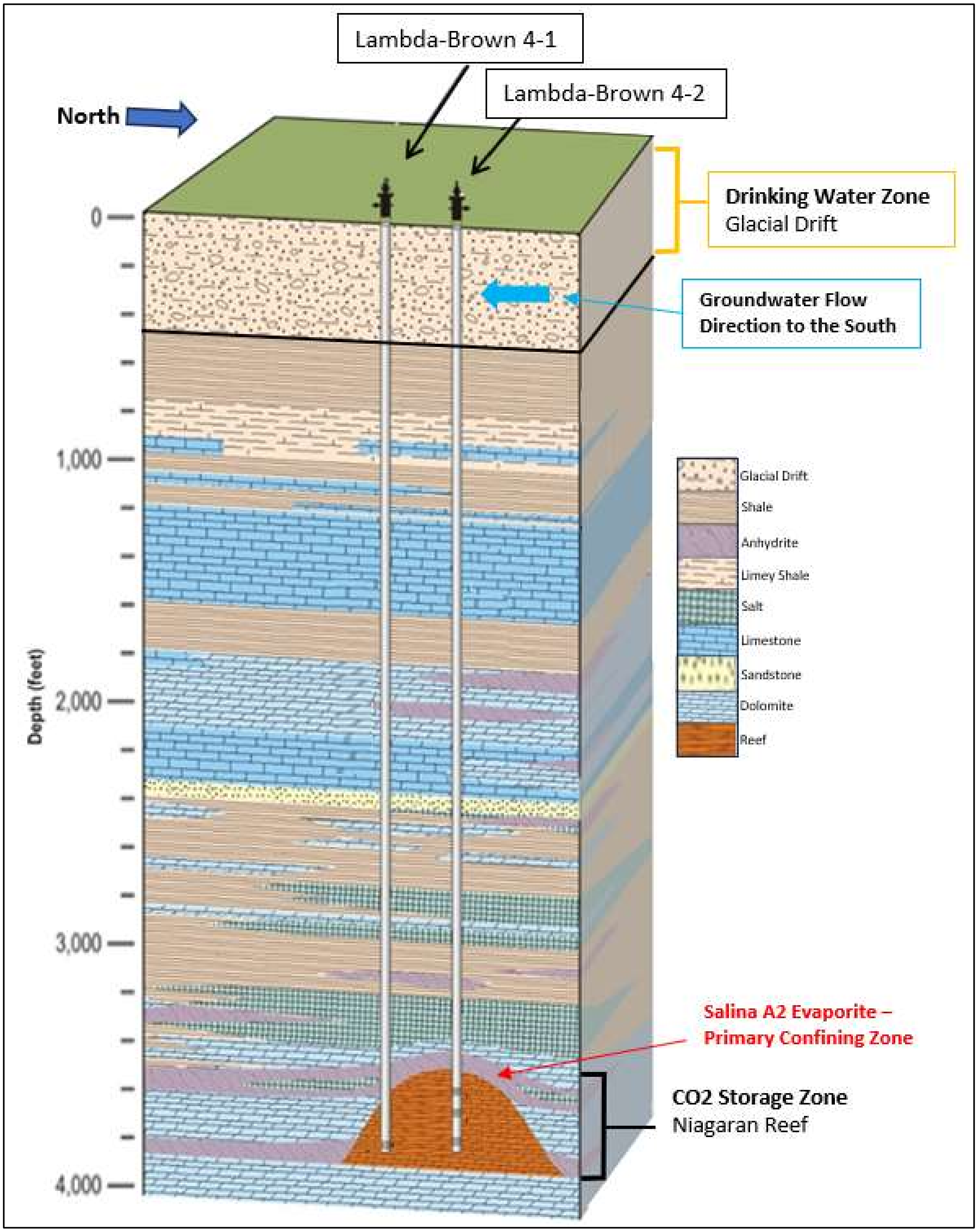

Figure 27: Cartoon cross section of Brown 4 reef showing relationship of injection zone vs groundwater drinking zone.

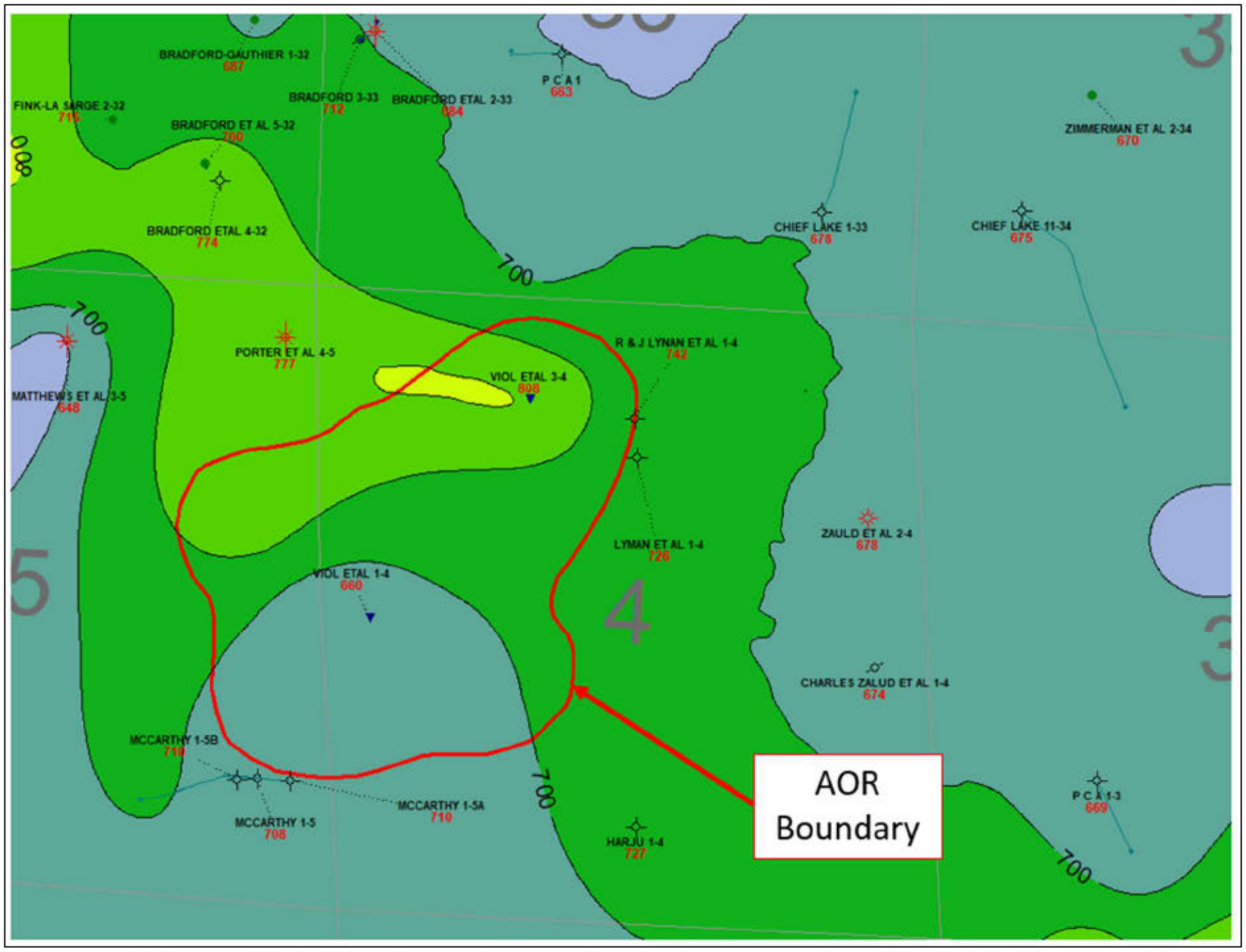

Figure 28: True vertical depth isopach map of groundwater aquifer (Glacial Drift) around AoR.

Table 12: Vertical distance separating USDW and injection zone

Well Name	Base of USDW, TVD ft	Top of Injection Zone, TVD ft	Vertical Distance Separating, TVD ft
Viol 1-4	662	4,316	3,654
Viol 3-4	814	4,300	3,486

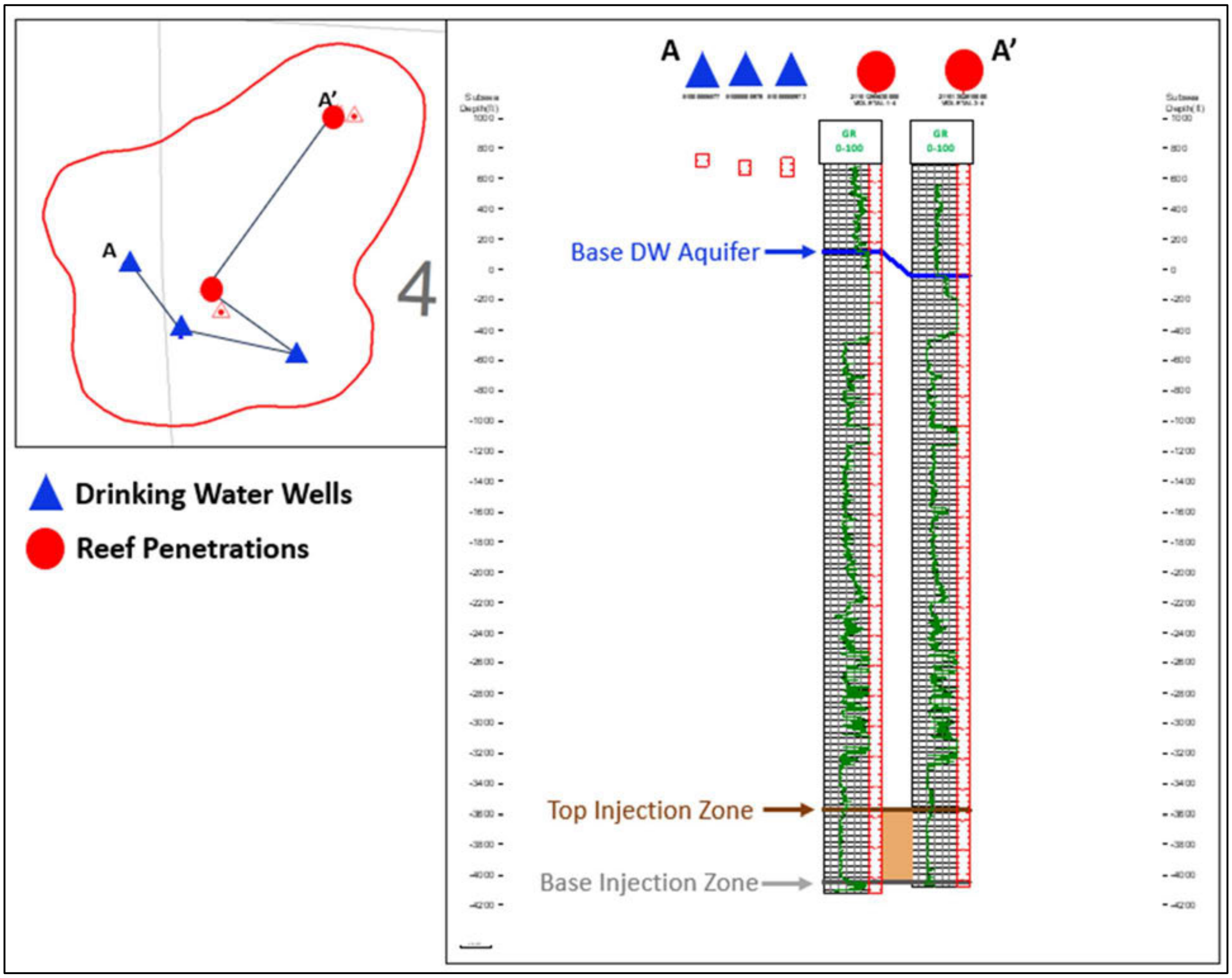

Figure 29: Cross section through drinking water and production wells in the Brown 4 AoR.

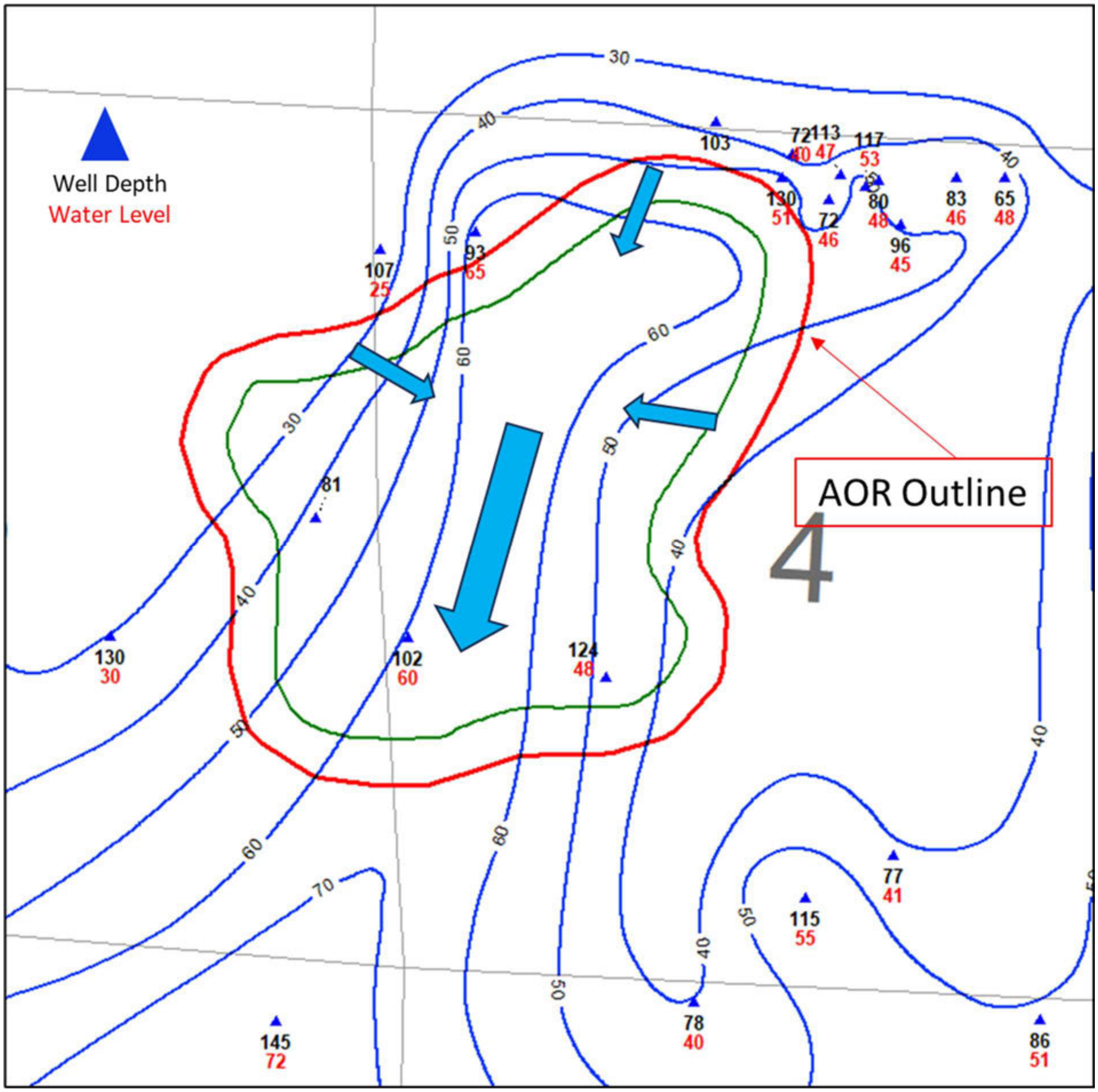

Figure 30: Groundwater flow map derived from data in surrounding water wells.

Geochemistry [40 CFR 146.82(a)(6)]

Lambda does not anticipate that significant levels of geochemical reactions will take place in either the injection zone or confining zone. The Brown 4 reef is a depleted natural gas reservoir with a connate water saturation of approximately 11%. The primary pore space to be filled by CO_2 sequestration is occupied by low pressure natural gas yielding minimal geochemical interference.

Ongoing CO_2 injection operations have been and are being implemented across the NRT over the past decade with no indication of alterations due to geochemical reactions with CO_2. Degradation of porosity and permeability due to mineralization is typically unique to saline aquifer sequestration zones. This geochemical process has a significantly lower effect on low water saturation, depleted hydrocarbon reservoirs such as the Brown 4 GSP. The primary mineralization risk associated with CO_2 injection into the Brown 4 reef is the dissolution of limestone, caused by the formation of carbonic acid resulting from the mixing of CO_2 with reservoir water. The result of this reaction has been documented to affect both porosity and permeability of the carbonate storage complex. However, work conducted by Grgic (2011) and Saaltink et al (2013) found that dissolution of calcite at a large (field) scale would be low due to the effects of carbonate buffering. An increase in the acidity of the pore fluid leads to the dissolution of calcite. However, this process utilizes free protons in solution, leading to an increased pH of the interstitial water, thereby balancing the system. Another factor that significantly reduces the risks associated with the $CaCO_3$ dissolution is the reduced solubility of CO_2 with decrease pressure. Under initial injection conditions, the reservoir pressure will be approximately 23 psia, indicating a significant decrease in the solubility of CO_2 in water. This suggests that a field-level equilibrium will be established well before noticeable increases in pressure are observed (Van Der Meer 2005).

Due to the current depleted state of the Brown 4 reservoir, the water in the reef is immovable, and as such Lambda is unable to collect a sample. Thus, Lambda has utilized a typical water analysis obtained from wells that produce free water in the NRT.

Table 13: Results of Niagaran water geochemical analysis. The water density is Claimed PBI [redacted].

Components	Value (mg/L)
Claimed as PBI [redacted]	[redacted]
[redacted]	[redacted]
[redacted]	[redacted]
[redacted]	[redacted]
[redacted]	[redacted]
[redacted]	[redacted]
[redacted]	[redacted]
[redacted]	[redacted]
[redacted]	[redacted]
[redacted]	[redacted]
[redacted]	[redacted]
[redacted]	[redacted]
[redacted]	[redacted]
[redacted]	[redacted]
[redacted]	[redacted]

The gas composition for the Brown 4 reservoir was determined using gas chromatography, method GPA 2261M. Figure 31 shows the results of the gas analysis for the Viol 1-4 well within the AoR. Gas composition analysis was routinely completed upon reservoir discovery and was collected across the field.

Claimed as PBI

[redacted]

Figure 31: Gas analysis from Viol 1-4 in Niagaran Brown 4 formation.

Other Information (Including Surface Air and/or Soil Gas Data, if Applicable)

A baseline vegetation survey will be conducted prior to construction, and Lambda will repeat the survey annually. Vegetation will be monitored during the early and late growing seasons at several points representing the various plant communities in the AoR, as access allows. Signs of stress will be documented and compared year-to-year via photographs and aerial imagery. Other potential sources of stress such as weather conditions, insect infestations, logging, etc. will also be documented. Plant health in the AoR will be compared to that in the surrounding area.

Site Suitability [40 CFR 146.83]

Storage capacity for the Brown 4 storage reservoir based on computational modeling results is up to [redacted] of CO_2. This is sufficient capacity for the total proposed injectate volume. Lambda is positioned for successful permanent CO_2 sequestration for the following reasons:

1. NRT reservoir hydrocarbons were confined for several hundred million years.
2. Comprehensive geological studies of over 50 years of development in the NRT shows the reefs are fit for secure storage as individual, isolated reservoirs based off of actual historical measurements of pressures and reservoir conditions within each reef.
3. Lambda plans to limit maximum bottomhole injection pressure to the original reservoir pressure during sequestration operations, which is below 90% of the reservoir fracture pressure.
4. Multiple reefs within the NRT are currently being utilized for commercial natural gas storage with approved injection pressures above original reservoir pressure, indicating a wide safety margin for the Brown 4 proposed maximum injection pressure.
5. Lambda utilized field production and pressure data history to match the energy of the storage complex. By achieving an accurate match to historical pressures, Lambda can assert with a very high degree of confidence that the reef is not capable of transmitting a fluid into a laterally adjacent formation.
6. The pressure history data of the reef constitutes a long-term negative pressure test. The reservoir pressure has been depleted by ~99% from original value (from 2,442.8 psia to 23 psia) for the last 49 years with no increase that would indicate an influx of fluid from adjacent formations (Figure 32).
7. Historical pressure data from nearby reefs show a lack of communication between the reefs, further proving that each reef is an individual system that will contain injected CO_2 up to original reservoir pressure (Figure 33).
8. Extensive operational knowledge through the long history of NRT development provides confidence in the ability to inject and securely monitor with experienced personnel and proven equipment.
9. Broad existing infrastructure with minimal additional construction impact provides nearly immediate capture capability.
10. Computational modeling shows final CO_2 concentrations fully contained within the boundary of the Brown 4 GSP for the entirety of injection and remaining at least 100 years post injection (Figure 34).

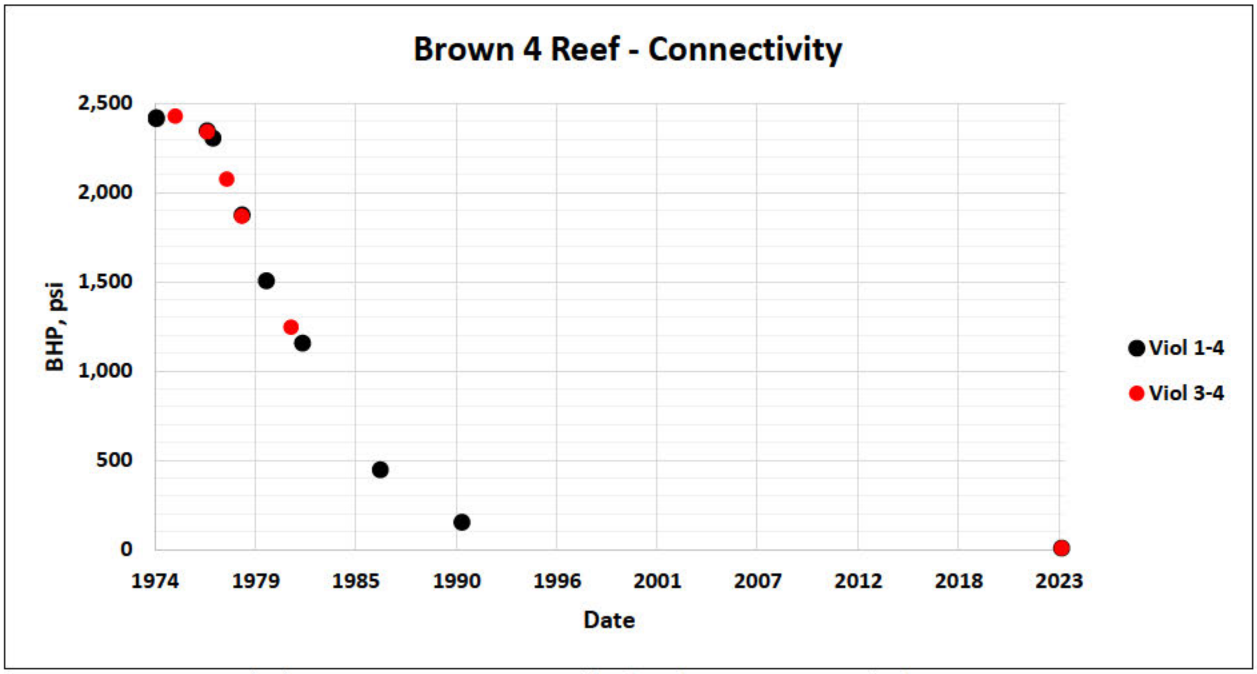

Figure 32: Bottomhole pressure versus time (hydraulic connectivity) showing consistent pressure trend and high connectivity between the wells within the Brown 4 reef.

Claimed as PBI

[redacted]

Figure 33: Static pressure plots seen in Figure 11 showing pressure isolation between of surrounding reefs.

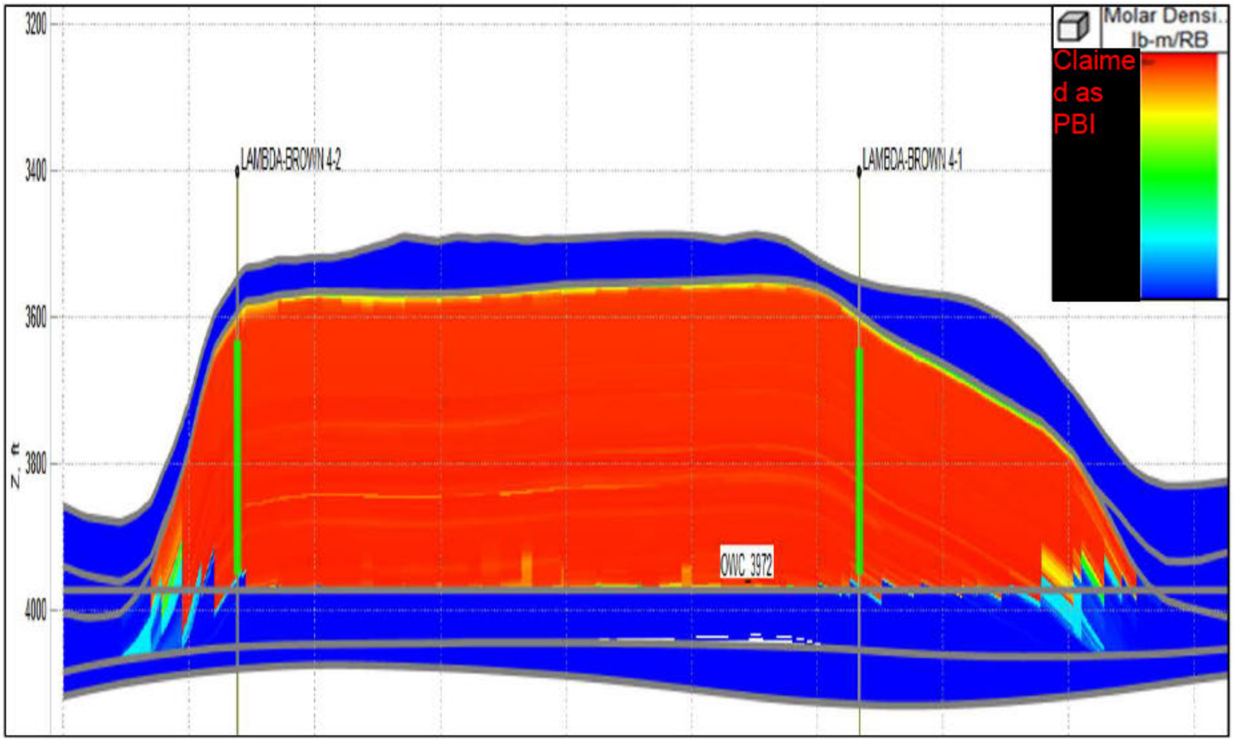

Figure 34: Cross section showing the CO_2 concentration within the reef 100 years post injection.

References

Barnes, D., Harrison, B., Grammer, G. M., & Asmus, J. 2013. CO_2/EOR and Geological Carbon Storage Resource Potential in the Niagaran Pinnacle Reef Trend, Lower Michigan, USA. Energy Procedia, 37, 6786-6799.

Barree, R. D., V. L. Barree, and D. Craig. 2007. Holistic Fracture Diagnostics. SPE Rocky Mountain Oil & Gas Technology Symposium. SPE-107877-MS.

Briggs, L., Briggs, D., Elmore, D., and Gill, D., 1978, Stratigraphic Facies of Carbonate Platform and Basinal Deposits, Late Middle Silurian, Michigan Basin, The North-Central Section of the Geological Society of America Field Excursions: New York, Geological Society of America.

Castillo, J. L. 1987. Modified Fracture Pressure Decline Analysis Including Pressure-Dependent Leakoff. SPE Low Permeability Reservoirs Symposium. SPE-16417-MS.

Core Energy. 2018. Northern Niagaran Pinnacle Reef Trend (NNPRT) CO_2 Monitoring, Reporting and Verification (MRV) Plan. https://www.epa.gov/sites/production/files/2018-10/documents/coreenergyniagaran_mrvplan.pdf.

De Bree, P. and J.V. Walters. 1989. Micro/Minifrac Test Procedures and Interpretation for In-Situ Stress Determination. International Journal of Rock Mechanics and Mining Sciences & Geomechanics Abstracts, Volume 26, Issue 6, Pages 515-521.

Gill, D. 1973. Stratigraphy, Facies, Evolution and Diagenesis of Productive Niagaran Guelph Reefs and Cayugan Sabkha Deposits, the Bell River Mills Gas Field, Michigan Basin. Unpublished Doctoral Thesis, University of Michigan, Ann Arbor, MI.

Gill, D. 1979. Differential Entrapment of Oil and Gas in Niagaran Pinnacle-Reef Belt of Northern Michigan. AAPG Bulletin 63, 608-620.

Grgic, D. 2011. Influence of CO_2 on the Long-Term Chemomechanical Behavior of an Oolitic Limestone, Journal of Geophysical Research, Volume 116, Issue B7

Huh, J. M. S. 1973. Geology and Diagenesis of the Niagaran Pinnacle Reef in the Northern Shelf of the Michigan Basin. Unpublished Doctoral Dissertation, University of Michigan, Ann Arbor, MI.

Jones, C. and J.P. Sargeant. 1993. Obtaining the minimum horizontal stress from microfracture test data: A new approach using a derivative algorithm. SPE Production & Facilities, SPE-18867-PA, Pages 39-44

Kelley, M., Haagsma, A., Champagne, P., Glier, J., Gupta, N., Yugulis, M.H., Hawkins, J., Main, J., Pasumarti, A., Sminchak, J., Weber, S., Mannes, B., Pardini, R., Sanders, K., Harrison, W., Goodman, W., Wade, S., Cunningham, S.L., Neal, J., Bacon, D.H., Demirkanli, I., White, S.K., Carroll, S., Middleton, R., and Yaw, S.P. 2018. Integrated Pre-Feasibility Assessment for a

Northern Michigan Basin CarbonSAFE CO_2 Storage Complex. United States Department of Energy. https://doi.org/10.2172/1469190

Raziperchikolaee, S., Kelley, M., Moronkeji, H., Xu, D., Guillermo, B., and Pardni, R. 2019. Advanced Formation Testing Using a Wireline-Deployed Formation Testing Tool to Characterize In-Situ Parameters in a Depleted Niagaran Pinnacle Reef Carbonate Reservoir. U.S. Rock Mechanics/Geomechanics Symposium, ARMA-2019-1637.

Ritter, A. 2008. Evaluating the Controls of Reservoir Heterogeneity of Silurian Pinnacle Reefs, Michigan Basin. Unpublished Master's Thesis, Western Michigan University, Kalamazoo, MI.

Saaltink, M.W., Viarroasa, V., De Gaspari, F., Silva, O., Carrera, J., and Rotting, T.S. 2013. A Method for Incorporating Equilibrium Chemical Reactions Into Multiphase Flow Models for CO_2 Storage. Advances in Water Resources, Volume 62, Part C, pages 431-441

Van Der Meer, B. 2005. Carbon Dioxide Storage in Natural Gas Reservoirs, Oil and Gas Science and Technology, Volume 60, Number 3, pages 527-536